Quantum Chemical Studies of Proton-Coupled Electron Transfer in Metalloenzymes

Per E. M. Siegbahn* and Margareta R. A. Blomberg*

Department of Physics, AlbaNova University Center and Department of Biochemistry and Biophysics, Arrhenius Laboratory, Stockholm University, SE-106 91, Stockholm, Sweden

Received February 26, 2010

Contents

1. Introduction

Proton-coupled electron transfer (PCET) is a general name for a group of rather different reactions occurring in most redox-active enzymes. They all involve electron transfer from a donor to an acceptor, but the degree and character of proton coupling varies strongly from case to case. In the present text, the conventional use of the term PCET will be adopted, in which PCET stresses the fact that connected with an electron transfer (ET) there is a significant proton motion. PCET could be either a concerted one-step process or a two-step process in which there is a first step of ET followed by a second step of proton transfer. A different use of the term PCET exists, where it only stands for the concerted one-step process, but that definition will not be used here. For experimentally observed PCET reactions, the reader is referred to the comprehensive review by Huynh and Meyer.[1]

It is common to separate PCET reactions into different groups. The purpose of making a classification of the PCET reactions is to emphasize that enzymes have been adapted in quite different ways to the different types of these reactions. In one extreme, a proton and an electron are both transferred between the same donor and acceptor, more or less simultaneously. This type of reaction is here termed hydrogen-atom transfer (HAT). In the other extreme, the electron transfer occurs between one donor and one acceptor, while the proton transfer occurs between entirely different donors and acceptors and often not simultaneously to the electron transfer. This is a very common type of reaction

Per E. M. Siegbahn was born in Stockholm, Sweden. He did his undergraduate studies at Uppsala University and received his Ph.D. degree at Stockholm University in 1973 (with Björn Roos). He was a postdoctoral fellow at the University of California, Berkeley (with Henry F. Schaefer III), and at IBM, San Jose (with Bowen Liu). He returned to Stockholm and has remained ever since. His interests have varied over the years from the development of ab initio quantum chemical methods, to the applications on gas-phase reactions of small molecules, to models of heterogeneous catalysts, to the present interest in mechanisms for redox-active enzymes.

Margareta R. A. Blomberg received her Ph.D. degree in the field of quantum chemistry at the Department of Physics, Stockholm University, in 1983. After a postdoctorial period at the IBM San Jose research laboratory with Bowen Liu, she returned to Per Siegbahn's group at Stockholm University. Most of her scientific work has been devoted to the elucidation of reaction mechanisms of transition-metal systems. In recent years her research has focused on biochemical systems, in particular metalloenzymes.

* To whom correspondence should be addressed. P.E.M.S.: phone, +46-8-16 12 63; e-mail: ps@fysik.su.se. M.R.A.B.: phone, +46-8-16 12 64; e-mail: mb@fysik.su.se.

10.1021/cr100070p
Published on Web 08/02/2010

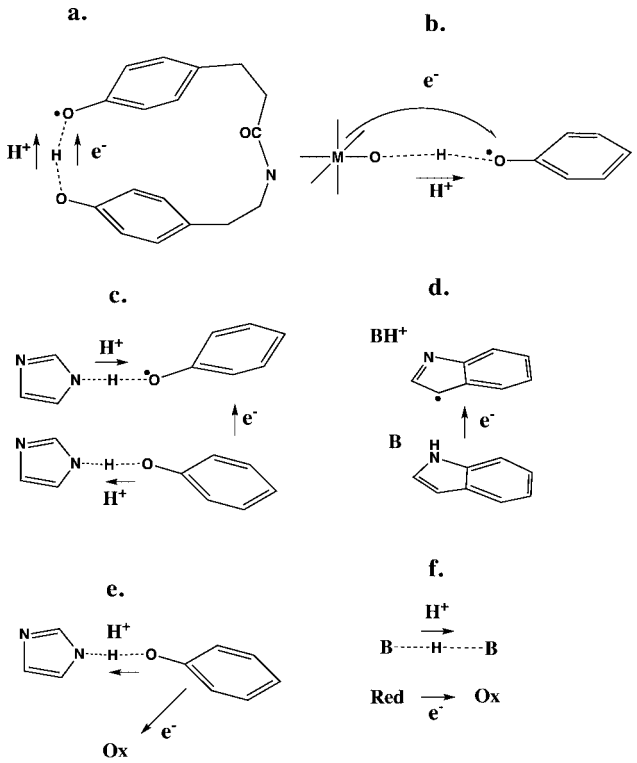

Figure 1. Different types of proton-coupled electron transfer. (a and b) Two cases of HAT discussed in the text: (a) found in RNR and (b) suggested for PSII. (c−f) Different cases of PCET: (c) found in RNR, (d) in RNR lyase, (e) in PSII, and (f) in CcO.

and will here be described with cytochrome *c* oxidase (CcO) (Figure 1f) and photosystem II (PSII) (Figure 1e) as examples. The group of HAT reactions can usefully be divided into smaller subgroups. In the first subgroup, see Figure 1a, the proton and electron are transferred between the same molecules. This is a common type of reaction step in many radical enzymes.[2−4] For long-range radical transfer, this type of transfer occurs, to our knowledge, only in ribonucleotide reductase (RNR) between two tyrosines and between a tyrosine and a cysteine in the radical transfer chain.[5] In the second HAT subgroup, see Figure 1b, the electron transfer occurs from a metal as donor to an amino acid acceptor while the proton transfer occurs to the same acceptor but from a ligand of the metal complex as donor. Reactions of this type (or its reverse) occur, for example, in RNR between Tyr122 and the iron dimer complex in R2, in methane monooxygenase (MMO) between the methane substrate and the iron dimer, and in many other enzymes. It has also been suggested to occur in PSII,[6] originally termed the hydrogen-atom abstraction model. It should be added that an H-atom transfer never involves a combined motion of a proton and its electron together in the strictest sense, since the moving proton has never been found to carry any significant spin at any point of the transfer. A quite different definition of HAT has been suggested where this term is restricted to cases where the proton and electron involve the same orbitals.[7] This more restricted definition may be more reasonable in other areas of chemistry, but in transition-metal biochemistry it would lead to the conclusion that the large class of reactions shown in Figure 1b would fall outside the HAT definition. This definition therefore does not appear to be very useful in the present context and will not be adopted here.

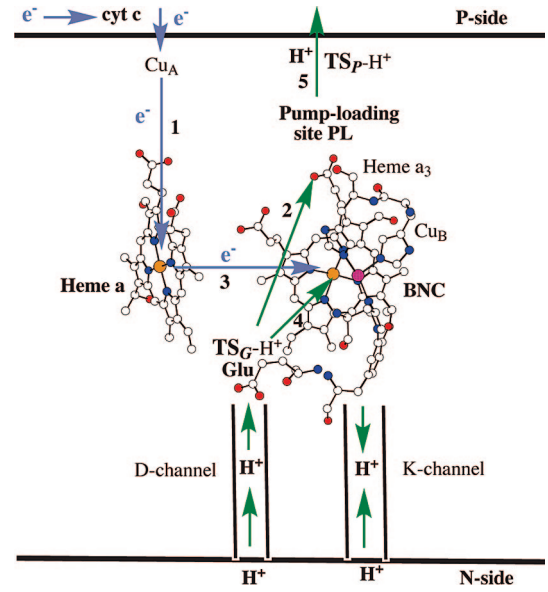

Figure 2. Overview of electron and proton transfer in cytochrome *c* oxidase.

Two other types of PCET are shown in Figure 1c and 1d. In Figure 1c, the electron is transferred between two phenol rings (as in tyrosine), coupled to a proton transfer shuttle involving a base and an acid, here illustrated by two histidines. The acid−base could obviously be water. This type of PCET has been theoretically demonstrated for radical transfer initiation in RNR[8] and experimentally for the same enzyme in a region of the radical transfer chain.[9,10] In Figure 1d, an electron transfer between two indol rings (as in tryptophane) hydrogen bonded to a base is shown. This type of transfer could as an extreme be a pure electron transfer, depending on the involvement of the base.

As mentioned above, a very important case of PCET occurrs in cytochrome *c* oxidase, the terminal enzyme in the respiratory chain, located in the mitochondrial (or bacterial) membrane. As depicted in Figure 2, the electrons and protons are here taken up from different sides of the membrane, i.e., the electron and proton donors are entirely different. Furthermore, each electron uptake is coupled to the uptake of two protons, ending up in different places, one in the binuclear center (BNC) for the chemistry and one on the other side of the membrane, building up a gradient. This requires a rather complicated scheme for the coupling, as indicated by the numbered arrows in Figure 2 for the different steps of intermixed electron and proton motion. A complicating factor is that the mechanism for coupling the electron and proton transfer has to work with a varying amount of electrochemical gradient across the membrane, corresponding to varying energetics for the individual steps. A further complicating factor is the fact that the final electron and proton acceptors are not identical in all steps. There are four different cases, due to the chemistry that occurs in the BNC. It should be emphasized that these very common PCET reactions are of the two-step type, where the electron and proton transfer processes are well separated. The electron is typically transferred first, leading to an intermediate (detectable or not) before the slower proton transfer occurs.

There has been a large amount of interest the past decade at a fundamental level to understand the quantum mechanical effects occurring in PCET processes.[11−13] These approaches are typically built on Marcus theory for electron transfer[14] with a goal to incorporate also proton motion into this theory.

The description is diabatic, in contrast to the conventional adiabatic treatment discussed in the present review. The treatment of the proton motion is quantum mechanical and not classical as in the examples discussed here. The diabatic approach has recently been analyzed and compared to the adiabatic approach.[15] It was concluded that the vibronic treatment in the diabatic approach may sometimes be a poor approximation in the range of regular donor−acceptor distances, which should be described by the adiabatic approximation. However, at long distances when the electronic coupling is small, the vibronic treatment provides a reasonable approximation. The conclusion that the diabatic approach is not strictly valid for most H transfers, now appears to be generally accepted.[16] In the adiabatic approach the accuracy is normally limited by the error of the potential-energy surface. At present, using the highest accuracy methods available, this error is usually not larger than 3 kcal/mol for a barrier height. This error translates to a factor of 10^2 on the rate (using transition-state theory). The error of the potential-energy surface is, of course, present also in the diabatic approach. The diabatic approaches have mainly been used to study tunneling, which have been shown to sometimes be of importance for isotope effects. However, a recent thorough analysis has shown that tunneling is usually of comparatively minor importance for catalysis and reaction mechanisms[17] and will therefore not be discussed further. It was concluded that a reaction barrier could typically be reduced from 15 to 14 kcal/mol by proton tunneling, which is within the accuracy limits of the calculated potential-energy surface.

In the diabatic approach, there has been a suggestion to define the difference between HAT and PCET based on the degree of electronic nonadiabaticity.[11] Just like in the alternative definition discussed above, where the orbitals involved were included in the definition,[7] this definition would lead to the conclusion that HAT does not exist in biological systems, except possibly in the tyrosine−tyrosyl case in RNR. For example, with this definition the hydrogen-atom transfer model suggested for PSII[6] will not be HAT but PCET. Since the difference between this HAT mechanism and the conventional PCET mechanism will be discussed here for PSII, the alternative definition will not be used here.

Cases of pure electron transfer (ET) will not be discussed much in the present review. They are only mentioned when they are the first step in a two-step PCET. In the cases when rates for ET are discussed they have been obtained either by experiments or by simple estimates based on Marcus theory.[14,18,19] The main effects determining the rate of ET have recently been summarized.[20] First, by far the most important factor determining the rate is the distance between the donor and the acceptor. At a much lower level of importance comes the driving force, which may be significant for uphill ET. Third, the reorganization energy can be used to control the rate but seldom affects the rate by more than 2 orders of magnitude. Fourth, the packing density of the protein medium can be important for long-distance transfer. Overall, the ET rate is rarely rate limiting since evolution can easily obtain a desired fast rate by changing the protein structure to move the donor and acceptor as close to each other as necessary.

2. Computational Methods

The most useful electronic structure method for treating large molecular systems during the past decades has been the hybrid DFT method with the B3LYP exchange correlation functional.[21] In spite of numerous attempts, the accuracy of this functional has been difficult to improve upon. The experience using the B3LYP functional for enzyme active sites containing transition metals was reviewed a few years ago.[22] As for other DFT methods, there are three major sources of error. The first one is the self-interaction error, which gives a nonzero contribution for the interaction of an electron with itself. The second error is due to the inherent single-determinant description which, for example, does not allow a proper dissociation of bonds in all cases. This deficiency is sometimes termed lack of static correlation or missing near-degeneracy effects. The lack of static correlation and the self-interaction error cancel to a large extent in most cases. In fact, it can be argued that the functionals are optimized for this cancellation. The third error is the lack of van der Waals interaction, which can lead to significant errors when large systems interact, such as for the binding in the chlorophyll dimer in the reaction center of photosynthesis. From numerous applications it has been realized that the most sensitive parameter in the hybrid DFT method is the amount of exact exchange in the functional. By varying this amount in the case of interest, a reasonable idea of the accuracy can be obtained.

There are essentially two different approaches to model enzymes. In one approach, a small quantum mechanical (QM) model is surrounded by a molecular mechanics (MM) part, usually describing the rest of the enzyme.[23,24] This QM/MM methodology using DFT has not so far been used to study PCET processes in enzymes to any significant degree. Instead, the most common approach in this context has been to use a cluster model,[25] where all atoms are described quantum mechanically. The models have been gradually increased with time and can now contain up to 250 atoms. To model the rest of the enzyme, a simple dielectric cavity with fixed dielectric constant (usually $\varepsilon = 4.0$) has most often been used.

To set up energy diagrams for general PCET processes, redox potentials and pK_a values have to be determined. Determining these values accurately is very difficult with any purely computational method, including the QM/MM approach, due to the change of charge. For the cluster model, dielectric effects are often quite large. For a neutral model they can be on the order of 20 kcal/mol even for a model of 200 atoms, and for a singly charged model they can be twice as big. Since the dielectric cavity method is a rather approximate approach, this means that the absolute results using the cluster model will be quite uncertain. Other procedures have therefore been used to estimate these values. The simplest approach is to relate the calculated values to some experimentally known value for a similar system and shift all calculated results with the difference between theory and experiment for that system.[26] For photosystem II and cyctochrome oxidase discussed below, another approach has been used.[26−30] Since the electron and proton donors are the same in all steps in these systems, a simple parametrization can be used to make the calculations reproduce the total exergonicity of one cycle. This exergonicity is obtained from the difference in redox potential between the electron donor and the acceptor. When only the sum of an electron and a proton uptake (or release) is considered, there is only one

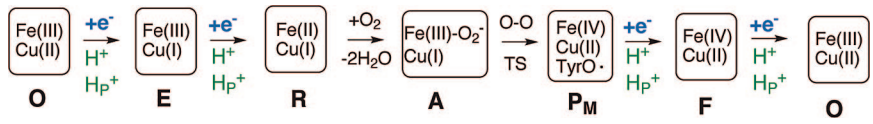

Figure 3. Sketch of the catalytic cycle in cytochrome *c* oxidase. H_P^+ represents protons pumped across the membrane.

unknown parameter, corresponding to the uptake (release) of a hydrogen atom (a proton and an electron). The energy levels calculated in this way are uniquely determined by the calculations and the total experimental exergonicity. Since all states obtained in this way have the same charge, the effect of the surrounding enzyme will be small and well described by the dielectric cavity model. It is normally also of interest to try to describe the individual steps of electron and proton transfer. To construct this type of energy profile, another parameter has to be introduced, dividing the cost of hydrogen-atom uptake (release) into the individual costs for the electron and the proton. In contrast to the first parameter, this second parameter is somewhat less well defined. However, for the systems discussed here the freedom of choosing this parameter is not very large. One simple criterion used for this second parameter is that the barriers for proton and electron uptake (release) should be minimized.

The binding of a H_2O molecule in bulk water is another energy that is difficult to calculate directly using quantum chemical models. In the energy diagrams discussed below an empirical value of 14 kcal/mol is used, taken from experience from numerous applications.[31,32] It can be added that even if the water molecule is taken or placed at a position where the binding energy is different from the one in the bulk, it is still the bulk value that should be used in the diagrams. For example, if a water molecule is taken from a position where it is more bound than 14 kcal/mol, this position would be immediately filled by another water molecule. A similar reasoning holds for the binding energy of an O_2 molecule, for which a free energy of 10 kcal/mol is used as an approximate value from the gas phase.

3. Cytochrome c Oxidase

Cytochrome *c* oxidase (CcO) in the respiratory chain is probably the enzyme where the coupling of electron and proton motion is most fascinating. The main reason this enzyme is so interesting from this perspective is that it is able to pump protons across the membrane without major structural changes and without ATP involvement. The pumping appears to be driven solely by the electrostatics of the electron motion, which may make it unique in biology. A major part of this review will therefore be spent on this enzyme, and the description will have to be quite detailed at some places to properly outline the function and mechanism. CcO has four redox-active metal centers as indicated in Figure 2. Two of those are used for electron transport only, a dinuclear copper center, Cu_A near the electron donor cytochrome *c* on the P side of the membrane, and a low-spin heme, heme a, in the interior of the protein. Near heme a the other two metal centers form a binuclear center (BNC) where the O_2 chemistry occurs. The BNC consists of another heme group, heme a_3 and a mononuclear copper complex with three histidine ligands and one cross-linked tyrosine, Cu_B.

The reduction of one O_2 molecule can be written

$$O_2 + 8H_N^+ + 4e^- \rightarrow 2H_2O + 4H_P^+$$

The four electrons are delivered via cytochrome *c* on the P side of the mitochondrial membrane, and the four protons needed to form the water molecules in the BNC are taken up from the N side of the membrane, via two proton channels, labeled the D and the K channel (see Figure 2). Coupled to this exergonic reaction another four protons are taken up from the N side and translocated across the entire membrane to the P side. Both the chemistry and the proton translocation contribute to the build up of an electrochemical gradient, in this way efficiently storing the energy, to be used by ATP-synthase making ATP. As mentioned above, the gradient will affect the energetics for electron and proton transfer to be discussed below.

In Figure 3, the four steps of the O_2 reduction are summarized. In each step an electron and a proton is taken up to the BNC for the chemistry, and one proton is translocated from the N side to the P side, also referred to as proton pumping. Almost all the processes in cytochrome oxidase can be described as proton or electron transfer reactions. What is most unusual compared to other systems is that the uptake of one electron is coupled to the uptake of two protons. To understand the mechanism for this proton pumping implies an understanding of how the different parts of one reduction step are organized and coupled to each other and how the protons are governed to move in the desired directions. In spite of extensive investigations using different experimental techniques during many years the mechanism for proton pumping in cytochrome oxidase remains one of the most intriguing questions in bioenergetics. In recent years it has become possible to apply quantum chemical methods to these questions, and it will be shown below how quantum chemical calculations in combination with experimental results can shed light on the different electron and proton transfer mechanisms in cytochrome oxidase.

3.1. PCET for Proton Pumping: One Reduction Step in Cytochrome Oxidase

One of the main goals in bioenergetics is to understand the proton-coupled electron transfer in cytochrome oxidase leading to the proton pumping. As mentioned above, the mechanism for this proton pumping is still far from understood, and many different mechanisms have been suggested based on various experimental observations.[33−42] It will be discussed below how different theoretical approaches can give new insights into the pumping mechanism, with special emphasis on the use of quantum chemical techniques. To adequately describe the different proposals, the description has to be rather detailed.

In an early attempt to use quantum chemistry to study the pumping mechanism in cytochrome oxidase, relevant pK_a values and redox potentials were calculated at the DFT level using rather limited models of the BNC.[26] Due to the limited

size of the models, the absolute accuracy of the calculations was not sufficient for drawing any definite conclusions about the pumping mechanism. Methods based on molecular mechanics and electrostatics are much faster than quantum chemical methods, and therefore, larger models can be used. Such methods have been applied to cytochrome oxidase, and in several studies important pK_a values at different levels of reduction have been calculated and various mechanisms for the proton pumping have been suggested.[43−48] In some studies quantum chemical methods have been used in combination with electrostatic methods, e.g., to evaluate pK_a values of possible pump-loading sites,[49−55] however with significantly different results for pK_a values of the same site at the same stage of reduction, showing that calculations of absolute pK_a values is a very difficult task. Monte Carlo simulation methods, allowing simulations over milliseconds for cytochrome oxidase,[56−58] have given insights into the electron-coupled proton transfer in the D channel, and possible pathways with barriers and thermodynamics have been constructed. On the basis of free-energy simulations a conformational gating of proton uptake in cytochrome oxidase has been suggested.[59] Recent results from kinetic experiments made it possible to construct energy diagrams for all parts of one reduction step,[60,32,61,62] and the analysis of these diagrams has led to different suggestions for the gating mechanism. One of the suggestions, based on simple electrostatics, is that a positively charged transition state is needed to prevent the pump protons to leak back to the N side.[60,32] Another suggestion, based on molecular dynamics simulations, is that it is a rotation of the Glu286 (numbering from *R. sphaeroides*) in the D channel that prevents the proton leakage, in combination with different dielectric constants for different parts of the active site in cytochrome oxidase.[62−64] Still another suggestion, also based on molecular dynamics simulations, is that it is the coupling between electron transfer and a reorientation of water dipoles that gives rise to the gating.[65,66] In summary, mainly methods based on molecular mechanics have been applied to try to localize the pump loading site and to find a gating mechanism to prevent proton leakage. Only very recently, quantum chemical methods have been used on large models to attack the actual gating mechanism,[67] and some of those results will be summarized below.

The mechanisms suggested for proton pumping in cytochrome oxidase, based on both experiment and theory, are different in many aspects, but there are also similarities. Several of the suggested mechanisms can be summarized in a standard model for proton pumping where the organization of the steps is based on electroneutrality and electrostatic interactions. The details of this model are illustrated in Figure 2 with arrows and numbers on the different steps. In step 1 an electron is transferred from cytochrome *c* via Cu_A to heme a. This raises the pK_a value of a pump-loading site (PL) in the vicinity of the active site, where the protons to be pumped are temporarily stored during the transfer across the membrane. The increased pK_a leads to a proton uptake from the N side via the D channel to the PL site in step 2. It is not known where the PL site is, but it is commonly suggested to be somewhere in the region of the propionates of heme a_3. In step 3 the electron is transferred from heme a to the BNC, since the proton in the PL site increases the redox potential of the electron acceptors in the BNC. The electron in the BNC in turn increases the pK_a of the proton acceptors in the BNC, and in step 4 the chemistry is completed by the uptake of a proton from the N side to the BNC. At this point the pK_a of the PL site is back to its lower value and the pump proton is expelled to the P side of the membrane in step 5. Essentially the same procedure occurs four times, one for each electron, with the main variation being that in one or two steps the K channel is used instead of the D channel for the proton involved in the chemistry. Also, due to the chemistry occurring in the BNC the energetics of electron and proton transfer to this site seems to be somewhat different in the different steps, as will be further discussed in section 3.2 below. This scheme can be considered as a mechanistic model for proton pumping, but it should be noted that there is no directionality in this model. There is nothing that prevents the protons to be taken up from the P side of the membrane instead of the N side, and there is nothing that prevents the pump proton to be expelled back to the N side when it is repelled by the proton in the BNC. In the beginning of the pumping process, with only a small membrane gradient, a thermodynamic gating might be possible but not when the gradient increases. Therefore, some type of kinetic gating is needed, and to describe that type of gating transition states need to be introduced, as will be discussed below.

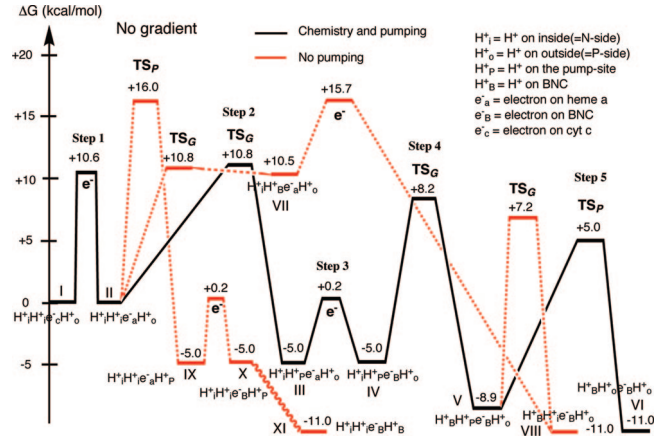

Figure 4. Energy profile for one reduction step in CcO (without gradient).

An important step forward to deepen and elaborate the picture of the proton pumping given above was taken with the recent kinetic experiment[68] for one of the reduction steps, **O** to **E** in Figure 3. In this experiment the time constants for the partial steps of electron and proton motion in the **O** to **E** step could be determined, and the interpretation made of the partial steps supports the standard scheme described above.[68] A general procedure is to use transition-state theory to convert such experimental time constants into barrier heights and construct an energy profile, which can be used to evaluate suggested reaction mechanisms in quantum chemical model calculations. In this case the procedure of setting up the energy diagram is complicated and can in itself lead to a better understanding of the process. Thus, a thorough analysis of the results from the kinetic experiment made it possible to construct an energy diagram that could fully explain the gating mechanisms in the sense that allowed reaction pathways, i.e., leading to both chemistry and pumping, at all branching points have lower barriers than the forbidden reaction paths not leading to pumping,[60,32] see Figure 4. The entire energy diagram corresponds to one of the four major steps in Figure 3, and the five substeps indicated in Figure 2 are indicated also in Figure 4. Clearly, only the allowed paths can be deduced from the kinetic

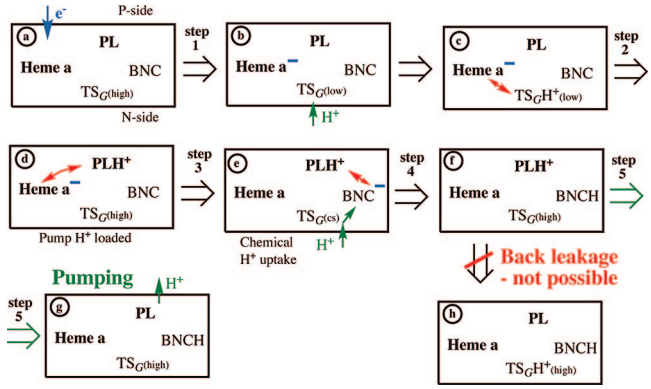

Figure 5. Scheme for the proton pumping in CcO, highlighting the electrostatic mechanism for gating protons toward the P side of the membrane. The red arrows indicate a mutual electrostatic stabilization.

experiments, and a similar diagram containing only the allowed pathways was constructed in ref 61. The forbidden pathways in Figure 4 will be be discussed below. The analysis of the experimental information involves an interpretation of the barriers in the energy diagram as corresponding to the transition states needed to obtain a kinetic gating mechanism for the proton motion. This analysis shows that at least two transition states are needed to fully understand the proton pumping: one between the P side of the membrane and the PL site, labeled TS_P in Figure 2, and one in the D channel, labeled TS_G in Figure 2. The correspondence between these transition states and the different barriers is also indicated in the diagrams in Figure 4. The exact location of the TS_P is difficult to guess, but for the TS_G different suggestions have been made. One proposal, to be discussed below, is that TS_G is located at or near the Glu286 at the end of the D channel.[60] TS_P has to be high enough to prevent protons from entering from the P side and low enough to allow the pump protons to pass when they are expelled to the P side. TS_G, on the other hand, has to be low enough to allow the protons to enter from the N side to both the PL site and the BNC but also high enough to prevent back flow from the PL site when the chemistry is completed and the pump proton should be expelled to the P site.

To construct the forbidden pathways in Figure 4 and to further develop the pumping mechanism assumptions had to be made also about the character of the transition states involved. Such assumptions also made it possible to construct models for quantum chemical calculations to evaluate the suggestions from the initial analysis using simple electrostatics[60,32] or dynamics simulations.[62−64] As it turned out, the most intricate transition state to describe is TS_G, and in refs 32 and 60 it was suggested that the only way to prevent back flow of protons from the PL site to the N side is to assume that this transition state should have a positive character as illustrated in Figure 5, emphasizing the electrostatic interactions. The boxes describe different states during one reduction step, and the five substeps discussed above are also indicated. One important state is shown in box **c**, where the electron on heme a stabilizes a positively charged TS_G, allowing the proton to enter from the N side to the PL site with a low barrier. This corresponds to step 2, going from II to III in the energy diagram in Figure 4. At this point, TS_P is higher in energy than TS_G, preventing protons from entering from the P side, corresponding to step II to IX in the energy diagram. The next important state is shown in box **f**, showing that when there is no negative charge near TS_G this barrier will be high, preventing the back flow of the protons at the PL site, step V to VIII in the energy diagram. At this stage the TS_P barrier is lower than the TS_G barrier, allowing the protons to be pumped, step 5, going from V to VI in the energy diagram. As mentioned above, one suggestion for the location of TS_G is Glu286, which is known from experiment to have a high pK_a value, and it is therefore normally protonated. A positively charged transition state for proton transfer from the N side of the membrane to the PL site could occur in such a way that the GluOH proton starts to move toward the PL site when a proton from the N side is already close to the Glu. The $GluO^-$ would therefore become immediately reprotonated.[32] However, there are many other suggestions for the pumping mechanism instead involving the transfer of the Glu286 proton to the PL site as the initial step, see for example refs 62−64. The quantum chemical calculations discussed below support the former mechanism with a positive transition state for proton transfer to the PL site and argue against an initial step that fully deprotonates the Glu286.[67] It should also be mentioned that it was suggested that the situation for proton transfer via the Glu286 is rather different when the electron has moved from heme a to the BNC.[32] The proton transfer to the BNC under this condition can occur via a transition state with more charge separation character, i.e., the Glu286 proton can move further away toward the electron in the BNC before the Glu286 is reprotonated by the next proton in the D channel; see further discussion in ref 32.

Most of the conclusions drawn from previous quantum chemical calculations on cytochrome oxidase were made by comparing models of the BNC of different size, as will be discussed in later sections below. Those calculations can only give indirect information on the pumping mechanism, such as the energetics of different steps of the catalytic cycle and O−O bond cleavage. Until very recently it was considered impossible to construct quantum chemical models that could give more direct information on the energetics of the pumping mechanism. Some preliminary results from DFT (B3LYP) calculations on large models consisting of about 250 atoms[67] will be summarized here. The purpose of those calculations was to start to evaluate the different suggestions for the gating mechanism, such as a positively charged transition state,[60,32] as compared to a transition state determined by different dielectric constants in different regions of the active site.[62] The energetics of the observed reaction paths in the diagram in Figure 4 were used as a calibration of the accuracy of the calculations. Most steps in this energy diagram correspond to proton transfer, and to obtain energetics for such processes pK_a values have to be calculated. Fortunately, it is enough to compare relative pK_a values, which can be calculated with a reasonable accuracy. The most important sites for which pK_a values are needed are the heme a_3 propionates and Glu286, which were therefore included in the model. Since an important aspect of the proton-pumping mechanisms suggested is the coupling between the electron transfer to heme a and the proton transfer to different sites, it was also necessary to include heme a in the model. To make these calculations possible it had to be assumed that the full BNC did not need to be included in the model but could be described as a positive charge (Cu(I)). One of the structures studied is depicted in Figure 6. The surrounding protein not included in this model

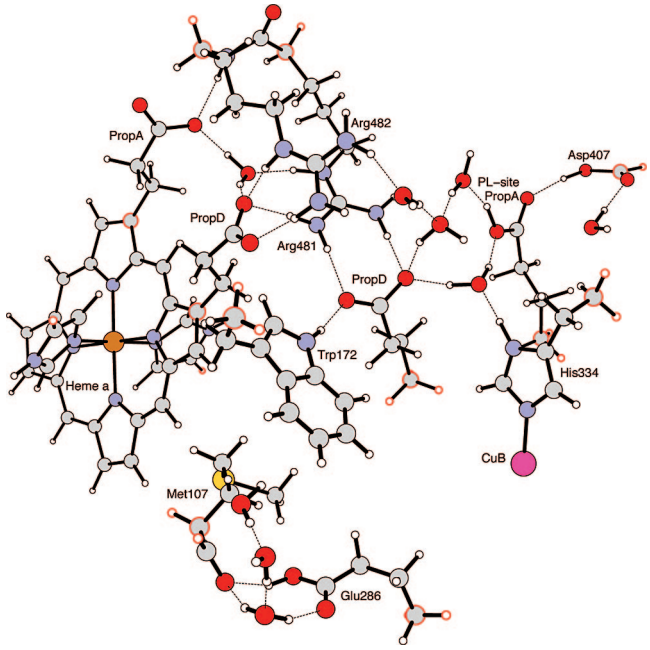

Figure 6. Model used to calculate relative pK_a values in CcO. The red circles indicate atoms fixed from the crystal structure.

was described as a dielectric continuum, with a dielectric constant of 4.0.

A corner stone in the standard pumping mechanism mentioned above is the coupling between the electron transfer to heme a and the uptake of a proton to the PL site. From the results of the kinetic experiments[68] it has been estimated that the pK_a value of the PL site increases by 5−7 kcal/mol (1 kcal/mol corresponds to 0.7 pK_a units) when heme a is reduced;[32,60−62] see also Figure 4. Using the model shown in Figure 6, the pK_a value of PropA (taken to be the PL site) was calculated with heme a oxidized and reduced, and the effect of the electron was found to be an increased affinity for the proton of 3.5 kcal/mol. This value is in reasonable agreement with the experimental observation that a proton is taken up when heme a is reduced. The reason the calculated effect of the electron is a bit small might be limitations in the model or that the best PL site was not found.

The model shown in Figure 6 could also be used to evaluate the suggestion that the initial step in proton pumping is a deprotonation of Glu286, with the proton moving to the PL site. This process, moving the proton from Glu286 to PropA, was from the calculations found to be endergonic by about 8 kcal/mol with heme a reduced, indicating that such a reaction step is not very likely.

Most importantly, the model in Figure 6 was used to evaluate the character of the transition state (TS_G) for proton transfer to the pump site, PL, i.e., for step 2, going from II to III in the diagram in Figure 4. One suggestion was that TS_G is located near Glu286 and is positively charged.[32,60] A positively charged transition state corresponding to TS_G between intermediates II and III in Figure 4 was modeled by adding a proton to the water cluster near Glu286. The energy of this transition-state structure was compared to the energy of the product structure (III) for this reaction step, which corresponds to moving the proton from the Glu286 region water cluster (TS_G) to the PL site (assumed to be PropA). During this proton uptake reaction step, II to III, heme a is reduced. The energy difference between these two structures (TS_G and III) taken from the experimental observations (see the diagram in Figure 4) is 16 kcal/mol. The corresponding calculated energy difference using the model in Figure 6 was found to be about 19 kcal/mol, showing that this type of transition state gives good agreement with the experimental observation for the allowed reaction path for the proton uptake. Most interesting is the evaluation of this type of positive transition state at TS_G on the forbidden path between intermediates V and VIII. Here back-leakage of the protons to the N side has to be prevented, when heme a is oxidized and the chemistry at the BNC is completed. Such a barrier was previously estimated based on simple electrostatics to be 16 kcal/mol;[32,60] see Figure 4. This barrier height corresponds to the energy difference of the same states discussed above, the protonated water cluster near Glu286 and the protonated PropA, but now with heme a oxidized. The calculations on the model in Figure 6 gave about 20 kcal/mol for this energy difference, thus essentially the same as with heme a reduced, and high enough to prevent back-leakage. These results show that the idea of a positively charged transition state near Glu286 can provide a working gating mechanism in cytochrome oxidase.

Furthermore, the idea that a neutral transition state can prevent back-leakage of the protons due to a difference in dielectric constant between the PL site and the TS_G was also evaluated using the model in Figure 6. In ref 62 a gating mechanism was suggested based on the assumption that the dielectric constant in the PL region is about 4 and in the TS_G region about 30. Using Coulomb's law and the distance between PropA and heme a (Fe) the quantum chemically calculated effect of the heme a electron on the pK_a value of PropA gave an effective dielectric constant of about 7, in reasonable agreement with previous suggestions.[32,60] Furthermore, the calculations on the corresponding effect of the heme a electron on the pK_a value of Glu286 gave an effective value of about 5 for the dielectric constant in this region, indicating that the dielectric constant should be rather similar at different parts of the active site. It can be noted that in these calculations the water molecules become oriented to optimize the hydrogen bonding, which turns out not to change very much between the two situations, with and without an electron in heme a.

Finally, a few comments can be made on the correlation between the proton-pumping mechanism and the structure of the cofactors in cytochrome oxidase. From the pumping mechanism described above it is clear that the PL site must be close to heme a to be enough affected electrostatically by the reduction of heme a to initiate the proton uptake. It is also clear that the PL site must be closer to the BNC with heme a_3 and Cu_B than to heme a, since in this way the reduction potential of the BNC is more affected by the protonation of the PL site than heme a, which leads to the electron transfer from heme a to the BNC. These conditions are fulfilled if the PL site is PropA on heme a_3 and if heme a and heme a_3 (BNC) are close in space. A side effect of this organization is that the proximity of the two heme groups leads to very fast electron transfer. However, this fast electron transfer is not necessarily needed for the functioning of cytochrome oxidase. The barrier between III and IV in Figure 4, which corresponds to this electron transfer, could probably be much higher without affecting the overall reaction.

3.2. PCET for the Entire Catalytic Cycle of Cytochrome Oxidase

To set up the energy profile of the **O** to **E** step, for which the kinetic experiments were performed, it was assumed that all four reduction steps in the catalytic cycle have the same exergonicity.[32,60−62] As mentioned above, the chemistry occurring in the BNC (forming two water molecules from molecular oxygen) makes the proton and electron acceptors in the BNC nonidentical for the four reduction steps. This implies that it is not obvious that the four steps actually will have the same energetics, so the assumption above was made for simplicity. However, since the exergonicity of the O_2 chemistry is used for the proton pumping across the membrane and cytochrome oxidase is known to be very efficient in storing the energy, it is still expected that the energetics should be quite similar in the four reduction steps. To better understand the pumping mechanism in cytochrome oxidase it is nevertheless important to elucidate the actual differences and similarities between the four reduction steps in Figure 3. Each step involves the uptake of one electron (from cytochrome *c*) and one proton (from bulk water on the N side), and at one level of description the total energy change of each reduction step can be determined as the sum of these two processes, corresponding to the uptake of a hydrogen atom. It can be noted that before the electrochemical gradient has begun to build up, there is no net cost for the proton translocation. To fully understand the processes in cytochrome oxidase, it is also of interest to know the energetics of all individual steps of proton and electron transfer to the BNC, thereby obtaining a picture of the coupling between the electron and proton transfer processes. For this purpose pK_a values and redox potentials for the BNC at different points of the reduction process have to be calculated and compared to the corresponding values for the electron and proton donors. As will be described below, it turns out that the coupling between electron and proton transfer to the BNC is complicated in itself, even without the requirement to achieve proton pumping.

Below it will be described how quantum chemistry has been applied to models of the BNC to calculate the energetics of the catalytic cycle of cytochrome oxidase.[26−30,69−71] As mentioned above, the energetics of electron and proton transfer in cytochrome oxidase are affected by the presence of the electrochemical gradient built up during the process. The quantum chemical modeling gives the initial energetics without the gradient, but the effects of the gradient can easily be applied on the calculated energetics.

One difficulty when calculating the energetics of the reduction steps of the catalytic cycle in cytochrome oxidase is to determine the cost for the uptake of the electrons and protons. In section 2 above one procedure to estimate these energies, which has been used in several studies of cytochrome oxidase,[26−30] was sketched. Using experimental redox potentials for the electron donor (cytochrome *c*, 0.25 V) and the ultimate acceptor (molecular oxygen, 0.8 V) and considering that four electrons are involved, the energy gain of one full cycle is about 51 kcal/mol (2.2 eV).[72] When only the sum of an electron and a proton uptake is considered each step can be considered as the formation of a new O−H bond and the hydrogen-atom binding energy is parametrized to fit the total exergonicity of 51 kcal/mol. To describe the individual steps of electron and proton transfer a second parameter has to be introduced, as described in section 2.

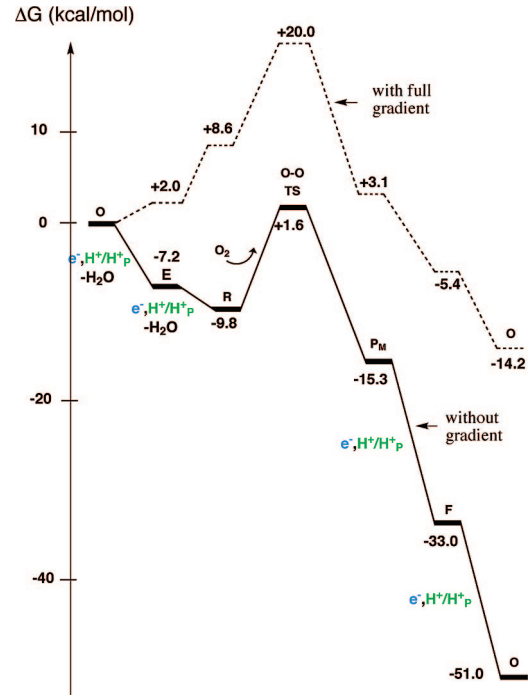

Figure 7. Energy diagram for dioxygen reduction in cytochrome *c* oxidase showing the transitions where both an electron and a proton are taken up. H_P^+ indicates that a proton is pumped across the entire membrane. The energies have been parametrized to give an overall energy of 51 kcal/mol. Tyrosinate is assumed to be present until the **R** state. The experimental O−O bond cleavage barrier is included.

Using models of the BNC (including the cross-linked tyrosine) the O−H bond strength of each of the four steps in the catalytic cycle can be calculated, and since there is no change in charge for the uptake of a hydrogen atom, this type of calculations is expected to give a rather good picture of the relative energetics for the four different steps.[28−30,70] The most recently published energy diagram constructed in this way is shown as the lower, full line curve in Figure 7.[30] Clearly this picture where each step is considered as a formation of a new O−H bond is somewhat too simplified, since the electron and proton are normally not going to the same part of the BNC. An important question is also to determine which position in the active site is protonated in each step, since the protonation pattern in the BNC has implications for the coupling between electron and proton transfer and for the pumping mechanism. The protonation sites are not so easily determined experimentally but are rather straightforward to investigate theoretically. An example of an energy diagram with all individual electron and proton transfer steps included is shown in Figure 8.[27]

Several similar diagrams as those presented in Figures 7 and 8 have been constructed using somewhat different models of the BNC for the quantum chemical calculations and slightly different parametrization procedures, the first one published in 2003.[26−29,70] The general picture obtained from all the different models except one[70] is the same; the energy release is significantly smaller in the reductive part of the cycle (**O** to **R**) than in the oxidative part (P_M to **O**), indicating that the energy release from the chemistry in the reductive part might be too low to afford pumping of one proton per electron in this part. Ideally all four steps should have about the same exergonicity, since the low exergonicity in some of the steps makes it difficult to construct a common pumping mechanism for all steps. The problem with the

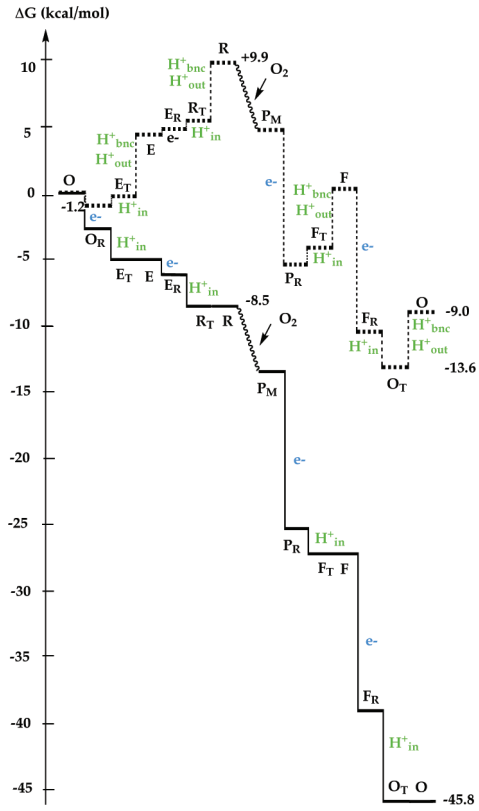

Figure 8. Energy diagram for dioxygen reduction in cytochrome *c* oxidase showing the individual steps of electron and proton transfer. Index T indicates that a proton has been taken up to the PL site. The energies have been parametrized to give an overall energy of 46 kcal/mol. Tyrosinate is assumed to be present until the **R** state. The O−O bond cleavage barrier is not included in this diagram.

uneven distribution of the energy over the catalytic cycle is better illustrated if the effects of the electrochemical gradient is taken into account. Starting from the calculated energy profiles just discussed, the effect on the energetics of the presence of a gradient could easily be evaluated. Since each of the four steps in the catalytic cycle corresponds to moving two charges against the gradient (including the pumped protons) and it is known from experiment that the maximum gradient is about 200 mV,[72] energy profiles shown as the upper, dashed curves in Figures 7 and 8 are obtained for the situation with full gradient. From these diagrams it can be seen that both steps in the reductive part of the cycle (**O** to **E** and **E** to **R**) become endergonic with full gradient. There is experimental evidence for the pumping of one proton per electron in the entire catalytic cycle, at least without electrochemical gradient. One possibility to decrease this endergonicity in the reductive part might be to avoid pumping in these two steps when the gradient increases. However, it is not trivial to construct a pumping mechanism where the pumping ceases due to a too low exergonicity while the chemistry still occurs. Therefore, it seems most likely to assume that these calculations do not give a completely correct picture of the energetics. In some studies[29,30] the results were improved in this respect by the introduction of a correction for the Fe(II) energy, based on a possible DFT error for the spin splittings of this state. A DFT problem could be part of the explanation, but since also the experimental redox potentials for the resting enzyme point in the same direction as the calculations,[73] it is likely that there is a problem with the description of the reaction steps. Some aspect of the active site in cytochrome oxidase is probably not taken into account, neither in the redox titrations on the resting enzyme nor in the theoretical modeling. Therefore, new calculations are needed, searching for better ways to describe the chemistry that occurs in the BNC.

It can be noted that in one of the studies,[70] published in 2007, the same energy steps as illustrated in Figure 7 were investigated, but the results from that study are rather different in the sense that the exergonicity of the two parts of the cycle, the oxidative and reductive parts, are much more similar to each other; see Figure 9 (following the path labeled "working", note that the energies in this figure are given in kJ/mol). The energy cost of electron and proton transfer is calculated in a different way in that study, but that should not affect the relative energies between the different steps. Comparing the results from ref 70 with the early results from ref 26, where a rather small model of the active site was used, it could be suspected that the differences in the calculated energetics were due to the different size of the models. However, the calculations in, e.g., ref 27, where larger models more similar to the one in ref 70 were used, gave essentially the same results for the energetics as in ref 26, showing that there must be some other explanation. Since the models and methods used are qualitatively very similar the most probable explanation to the differences in the results between ref 70, on the one hand, and refs 26−30, on the other hand, is that the calculations for certain intermediates have converged to excited states in at least one of these studies.

Another observation can be made from the results of the quantum chemical studies,[26−30] relevant for the coupling between electron and proton transfer to the BNC and which is partly connected to the problem with the low calculated energy release in the reductive part of the catalytic cycle. The calculations show that for some steps in the catalytic cycle there are two protonation sites with similar pK_a values: the tyrosinate formed when the P_M state is reduced and one of the oxygens coordinating to the metals. The electron transfer to the BNC triggers the proton transfer to the BNC by increasing its pK_a value (the pump protons are disregarded in this discussion). Clearly the next electron cannot be transferred to the BNC without the arrival of this proton, since the proton is needed to restore the higher redox potential of the BNC. The calculations showed that the two possible proton sites in the BNC, present in several reduction steps, do not affect the redox potential in the same way. Therefore, the only way to obtain high enough redox potentials in the BNC was to keep the tyrosinate unprotonated until the very last step in the cycle and at each one of the previous steps let the proton go to the metal−O sites in the BNC. Both diagrams shown in Figures 7 and 8 were constructed in this way. For the oxidative part of the catalytic cycle there was no problem with this procedure, since, as just mentioned, the two pK_a values are very similar, and the difference is within the uncertainty of the calculations. However, for the **O** to **E** step the calculated pK_a value for the tyrosinate is much larger than the one in the BNC, implying that the tyrosinate should be protonated already in this step. However, this would give a too low redox potential in the BNC with a very high barrier for the last electron transfer. At present there is no explanation to this problematic situation, occurring for many different models of the BNC, except that there might still be some aspect of the BNC missing in the models, leading to erroneous results for the

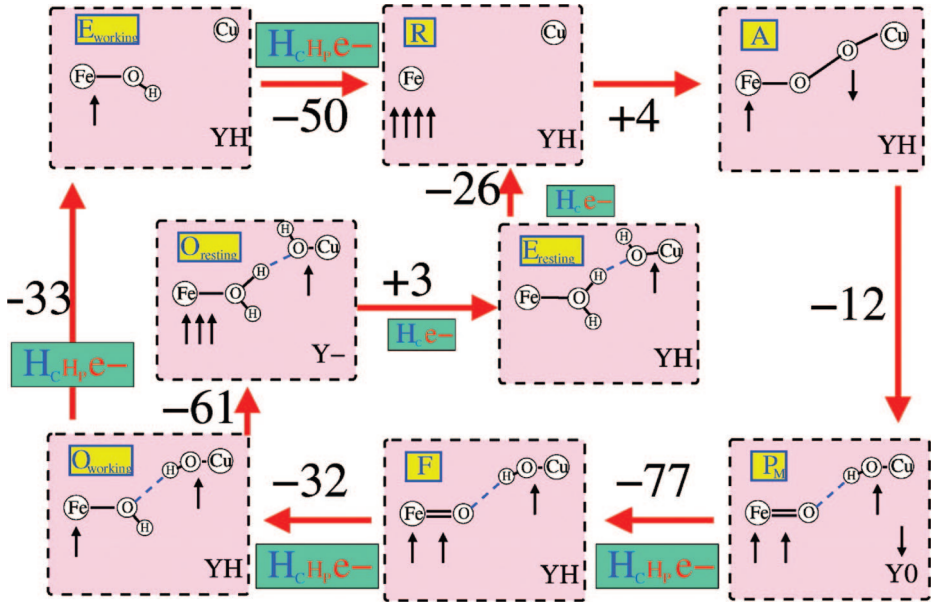

Figure 9. Calculated energies (in kJ/mol) for dioxygen reduction in cytochrome *c* oxidase showing the transitions where both an electron and a proton (H_C) are taken up.[70] H_P indicates a pumped proton. Reprinted with permission from ref 70. American Chemical Society Copyright 2007.

relative pK_a values, which might also be the source of the low energy release in the reductive part of the cycle discussed above. It can here be noted that in ref 70, which uses similar models and methods, a very different result was obtained for the protonation in the **F** to **O** step in the oxidative part of the cycle, see Figure 9, with a strong energetic preference of 15 kcal/mol (61 kJ/mol) for keeping the tyrosinate unprotonated, while in other studies the energy difference between the two possible protonation states of **O** was on the order of 3 kcal/mol.[26−30]

An extensive quantum chemical study of the entire catalytic cycle of a B-type cytochrome oxidase was published in 2008 by Fee and co-workers.[71] In that study several different DFT functionals were used to obtain a detailed description of the energetics of most partial steps of proton and electron transfer. A mechanism for proton pumping involving 14 different steps was suggested. In this mechanism a doubly protonated histidine residue hydrogen bonding to the PropA of heme a_3 is used as the pump loading site. In the A-type cytochrome oxidases this histidine coordinates to a magnesium ion, which is absent in the ba_3 enzyme modeled by Fee and co-workers. In that study the relative energies of different steps are calculated using explicitly calculated free energies for the electrons and protons transferred. Furthermore, pairwise comparisons of the energies were made in each of the predefined reaction steps without fully optimizing the structures. The energies are calculated by transferring protons from a "pH 7 bath" and removing the pumped protons into a "pH 3 bath". Energy diagrams constructed in this way are reproduced in Figure 10.[71] It can be noted that also in that study there seem to be some problems with the calculated energetics, since the energy diagrams in Figure 10 involve too high thermodynamic barriers to be compatible with the reaction rate of the enzyme.

The different steps of the catalytic cycle of cytochrome oxidase have also been studied using density functional theory (B3LYP) by Yoshioka and co-workers.[74−76] They, using partially optimized models of the active site, investigated the electronic structure of the main intermediates of the full catalytic cycle. However, since no energies were calculated, it is difficult to evaluate the suggested mechanisms. Also, the O−O bond cleavage step, to be discussed below, was studied in the same way, without energetics and without any attempts to find a transition state for the bond cleavage.

A very early attempt to use quantum chemistry to study the coupled electron and proton transfer in cytochrome oxidase was published in 2000.[69] Calculations were performed for the **O** to **E** and **E** to **R** steps using small models and methods with low accuracy (Hartree−Fock), which made it difficult to draw conclusions about the energetics of these steps.

Quantum chemical calculations have also been performed on models of the active site in cytochrome oxidase, trying to elucidate different properties of the BNC that might have relevance for the electron and proton transfer processes. For example, vibrational frequencies have been calculated in several studies,[77−79] and from one of those studies[79] it could be concluded that proton motion in the vicinity of the active site leads to changes in the vibrational spectra even without any change of the oxidation states of the metals. Another aspect of the active site in cytochrome oxidase is the presence of the somewhat unusual covalent bond between a histidine and a tyrosine, and it has been speculated that this cross-link might be important for the coupled electron and proton transfer process. The role of this tyrosine cross-link has therefore been addressed by quantum chemical calculations on models of the Cu_B complex alone.[80,81] The results in ref 81 were interpreted to show that the cross-link is important for the proton and electron affinities in the BNC and that this in turn could explain the presence of two pathways for proton uptake. In another study, quantum chemical calculations have been made trying to investigate reaction barriers in the less-established H path for proton transfer from the BNC to the P side of the membrane.[82] The results from the calculations on rather small models indicate reasonable barrier heights for proton motion along this pathway.

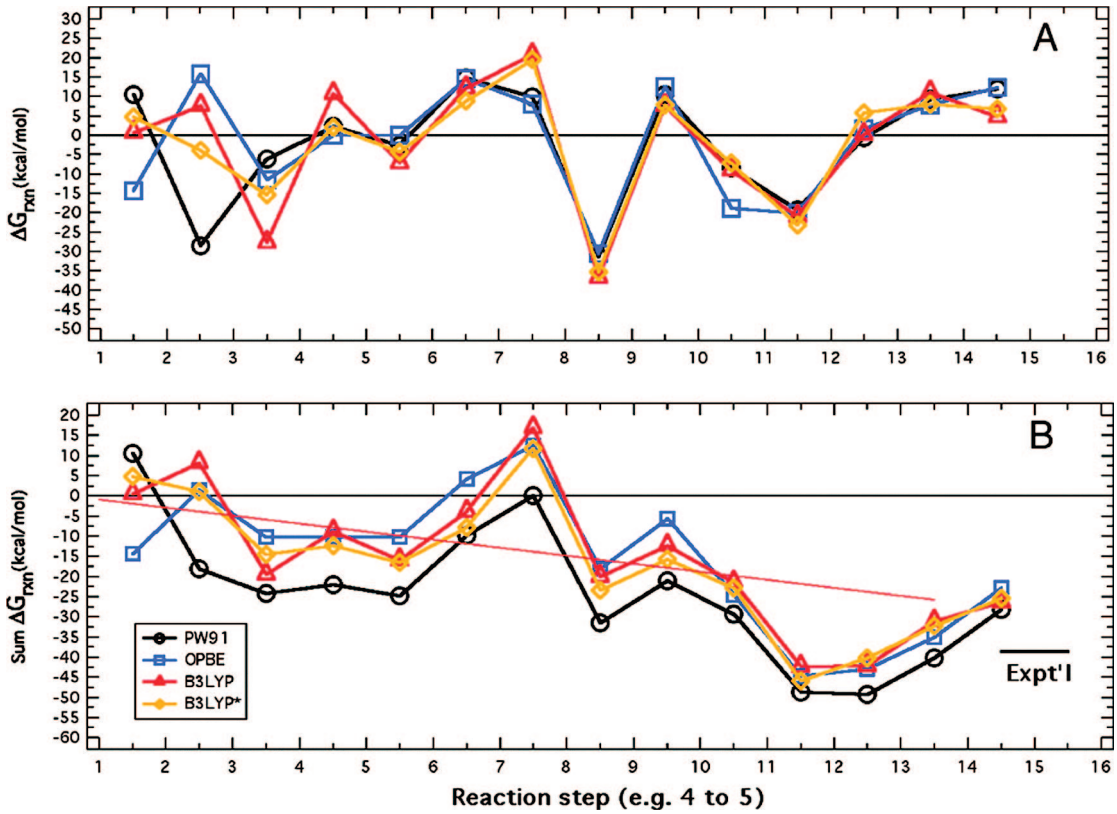

Figure 10. Energy diagram for dioxygen reduction in cytochrome *c* oxidase showing the individual 14 steps defined in ref 71: (A) energies of the individual steps and (B) cumulative sum of the energies. Reprinted with permission from ref 71. American Chemical Society Copyright 2008.

3.3. PCET for the O−O Bond Cleavage Step in Cytochrome Oxidase

The step in the catalytic cycle of Figure 3 not discussed so far is the O−O bond cleavage, starting with the two-electron-reduced **R** state, coordinating the oxygen molecule leading to compound **A**, from which the actual bond cleavage occurs yielding the P_M state. As indicated in Figure 3, these steps are not accompanied by any electron or proton uptake. On the other hand, the O−O bond cleavage is composed of several steps of internal electron and proton transfer, the coupling of which turns out to be rather difficult to describe. Several quantum chemical studies have been performed of the O−O bond cleavage in cytochrome oxidase,[27,29,30,74,83−85] and one model of the BNC used to study this step is shown in Figure 11.[30]

The picture of the O−O bond cleavage coming out from those studies is that the bond cleavage occurs in several steps. In connection with the formation of compound **A**, the oxygen molecule is reduced to a superoxide by one electron from iron, giving Fe(III) with low-spin coupling. The unpaired electrons on dioxygen and iron are antiferromagnetically coupled to an open-shell singlet. From isotope-labeling experiments it is known that one of the O_2 oxygens is bound to Cu after the bond cleavage, and since an oxo group on copper would be energetically unfavorable it has been suggested that the O−O bond cleavage leads to a hydroxyl group on copper.[86] When it was first observed that the O−O bond is cleaved already in the P_M intermediate, it was suggested that the electron needed for the bond cleavage came from the tyrosyl residue cross-linked to one of the copper-ligated histidines and that the formation of the hydroxyl group on copper involves a hydrogen-atom transfer from the tyrosine to the distal oxygen, forming a neutral

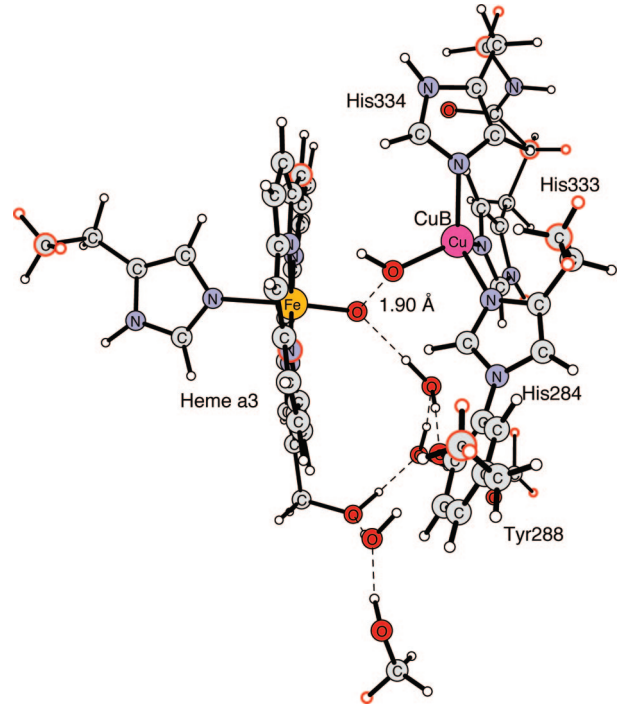

Figure 11. Structure of the optimized transition state for the O−O bond cleavage in cytochrome *c* oxidase. The red circles indicate atoms frozen from the crystal structure.

tyrosyl radical.[87] The quantum chemical calculations trying to explore this mechanism have given another picture. Starting from compound **A** as described above, the O−O bond cleavage occurs in two steps. In the first step the tyrosyl proton is transferred to the distal oxygen and at the same time an electron is transferred from Cu_B to the oxygens to

give a Fe(III)OOH peroxide, Cu(II), and a tyrosinate. In the second step the O−O bond is cleaved, and the tyrosyl electron is transferred to the oxygens, giving the Fe(IV)═O, Cu(II)−OH, TyrO· product. This second electron transfer step was found to be strongly dependent on the hydrogen bonding structure in the central BNC.[27,85] The experimental time constant for the disappearance of compound **A** corresponds to a total free energy of activation of 12.5 kcal/mol. However, the weak temperature dependence of the rate of P_M formation indicates that there is a large entropy effect on the activation energy of 6.1 kcal/mol, yielding an enthalpy barrier of only 6.4 kcal/mol.[88] Thus, the directly calculated activation energy, which corresponds to the enthalpy of activation, should be compared to the lower value of 6.4 kcal/mol, and the entropy effect should be added on top of this. Using several different models of the BNC it was found that already the first step, the formation of an FeOOH peroxide, is endothermic by 8−12 kcal/mol relative to compound **A**, depending on the model.[30] On top of this endothermicity, the O−O bond cleavage barrier was found to be between 8 and 12 kcal/mol (relative to the peroxide), resulting in a total enthalpy barrier between 16 and 24 kcal/mol, compared to the experimental value 6.4 kcal/mol, indicating that these coupled electron and proton transfer steps are not correctly described.[30]

The attempts to solve the problem with the high calculated barrier for the O−O bond cleavage have focused on the first step, the coupled electron and proton transfer to form the FeOOH peroxide. Early calculations showed that the addition of an extra proton to the active site lowers the activation energy for the O−O bond cleavage substantially,[83−85] but it was difficult to find a realistic site for such an extra proton in the BNC itself. More recent studies have identified the lysine, Lys362, in the K channel as the most likely site for an extra proton in the vicinity of the BNC. On the basis of electrostatic calculations it has been claimed that this lysine is neutral,[43,89] but more recent calculations[90] as well as experiment[91] indicate that it might be protonated. A protonated Lys362 would electrostatically stabilize a negatively charged tyrosinate and thereby the formation of the FeOOH intermediate. In contrast to the mechanism studied in the early quantum chemical calculations such a proton should not participate in the chemistry at the BNC. From the distance between Lys362 and Tyr288 (13 Å) a stabilization energy of 5−6 kcal/mol can be estimated (using $\varepsilon = 4$). A larger stabilization would be obtained if the lysine proton is allowed to move closer to the tyrosine when the tyrosine proton moves toward the dioxygen. Taking into account that the peroxide state is not observed experimentally and that the observed entropy effect on the activation energy for the O−O bond cleavage was considered most likely to occur between compound **A** with a loosely bound oxygen molecule and the more firmly bound peroxide FeOOH, it was estimated that the proton would have to move from the Lys362 about one-half of the way closer to Tyr288 to obtain a stabilization of the FeOOH peroxide state, strong enough to give a total free energy barrier in agreement with experiment.[30]

A completely different way to solve the problem with the endergonicity of the **A** to FeOOH peroxide step is to abandon the suggestion that the tyrosine proton is used to form the peroxide.[29] The peroxide proton could come from the D channel, like several protons do in later steps of the catalytic cycle, and the tyrosine proton could leave into the K channel to allow for the formation of a neutral tyrosyl radical. The motion of two protons in opposite directions would cancel each other and not be observable in electrogenic measurements. Therefore, such a mechanism would be in agreement with the experimental observation that the O−O bond cleavage step is not associated with significant proton motion perpendicular to the membrane. The energetics of this kind of mechanism is difficult to estimate; it can at present only be postulated that the peroxide formation would have to be endergonic by about 3 kcal/mol to give agreement with the experimental rate of P_M formation.

To make it possible to transfer the tyrosyl proton to molecular oxygen, as suggested in the original mechanism, at least one or two water molecules had to be added to the BNC, which in the early X-ray structures did not contain any water.[27,29,30,83−85] A difficulty there was to find the optimal number and positions of the added water molecules, which introduced some uncertainties in the modeling.[32] A recent crystal structure for the reduced state of cytochrome oxidase[92] contains several water molecules, and the uncertain positioning of water molecules can be avoided, still with similar results, as described above.[30]

4. Photosystem II

PCET in photosystem II (PSII) has many similarities to the ones in cytochrome *c* oxidase discussed above. This is obviously related to the goal of producing ATP in both systems. Since PSII is the only system in nature capable of forming oxygen from sunlight and water and since oxygen has played such a fundamental role for life on earth, a very large effort has been spent the past decades to understand this system. PSII is present in the thylakoid membranes of plants, algae, and cyanobacteria. The first X-ray structures of PSII were obtained only a few years ago and with a rather low resolution of 3.0−3.5 Å.[93−95]

Water oxidation in PSII has been studied by now nearly 10 years using hybrid DFT calculations. Three different theoretical approaches have been used, mostly for trying to obtain better structures than are available from experiments. In the first approach,[96] a cluster model of the OEC, was used with up to 200 atoms. In the second approach,[97] the QM/MM (quantum mechanics/molecular mechanics) methodology was employed. A relatively small QM part was surrounded by a large MM part, together making up the entire protein. In the third approach,[98] different models for the OEC were constructed based on the core topology derived by polarized EXAFS (extended X-ray absorption fine structure) spectra[99] and with a ligand structure chosen to fit reasonably well into the X-ray structure. On the basis of the agreement with experiments for the computed spin spectrum, the best candidates for the actual structure of the OEC have been selected. A comparison of these three approaches has recently been made, and it was concluded that the results of the cluster model are at present the most reliable ones.[100] Only the cluster approach has so far been used to study the energetics and other details of PCET for water oxidation. There have been many theoretical studies of PCET in the reaction center, see, for example, ref 101, but no quantum chemical study to out knowledge. Since this review concerns PCET, it will therefore only describe what has been obtained by the cluster approach for water oxidation.

The electron flow in PSII is schematically shown in Figure 12. The first event is that a photon ($h\nu$) enters the chlorophylls and the energy is transferred to the reaction center termed P_{680}. P_{680} is composed of four chlorophylls. At P_{680}

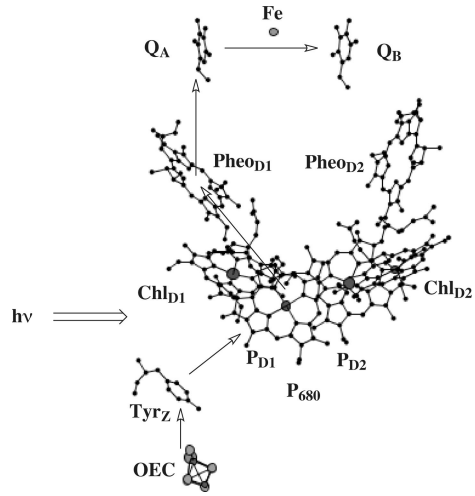

Figure 12. Schematic picture of electron flow in PSII.

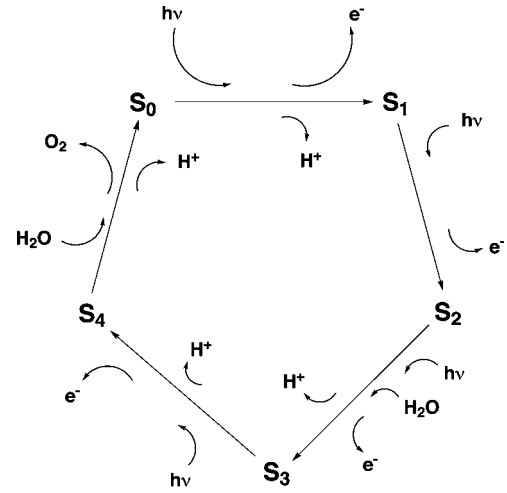

Figure 13. Kok S-state cycle for water oxidation; updated by recent research.

there will be a charge separation, with the electron rapidly transferred in a pure ET step to one of the pheophytins P*heo*$_{D1}$. The electron is then transferred further to the quinone Q_A in a somewhat slower step. In this process some energy generated by photoabsorption is lost as heat. This energy loss guarantees that the process is not reversed at the time scale of the water oxidation process. Q_A is furthermore sufficiently far away from P_{680} that the electron cannot go directly back by a shortcut in space. In a rather slow PCET step, the electron is finally transferred to a second quinone Q_B, which finishes the charge separation process.

The ionized P_{680}^+ has the highest redox potential known in biology with 1.25 V.[102,103] This potential is large enough to take an electron from a tyrosine, Tyr_Z, located in between P_{680} and the oxygen-evolving center (OEC). Tyr_Z is simultaneously deprotonated to a nearby histidine, His190, creating a neutral tyrosyl radical. In the key water oxidation step, an electron is then transferred from the Mn_4Ca complex of the OEC, where the substrate water molecules are bound, to the tyrosyl radical. Coupled to this oxidation of the OEC there will furthermore in most cases also be a transfer of a proton to the lumen (bulk water).

After four steps of the above process, each one requiring one photon of light, four electrons have left the OEC and four protons have left two substrate water molecules, leaving only their oxygens, which can form O_2. This is illustrated in the so-called Kok cycle shown in Figure 13. The intermediate S states have been directly observed spectroscopically and will be referred to in the text below.

The conventional mechanism for OEC oxidation is that the Tyr_Z radical acts as the electron acceptor, shown at the top of Figure 14 as PCET. The starting point of this mechanism is a Tyr_Z radical hydrogen bonded to a protonated His190. This is the immediate product of tyrosine oxidation by P_{680}^+. In this mechanism, the proton on His190 has therefore not been transferred further to the bulk before OEC oxidation.[104] At this point an electron is transferred from the OEC concertedly with a transfer of the His190 proton back to the Tyr_Z radical. The proton release to the lumen occurs from the water substrates at the OEC, see the bottom of the figure.

A quite different idea with a HAT mechanism for proton and electron abstraction from water in the dioxygen formation process was suggested about a decade ago by Babcock and co-workers[6] (see also next section). The starting point for HAT is different from the PCET one described above.

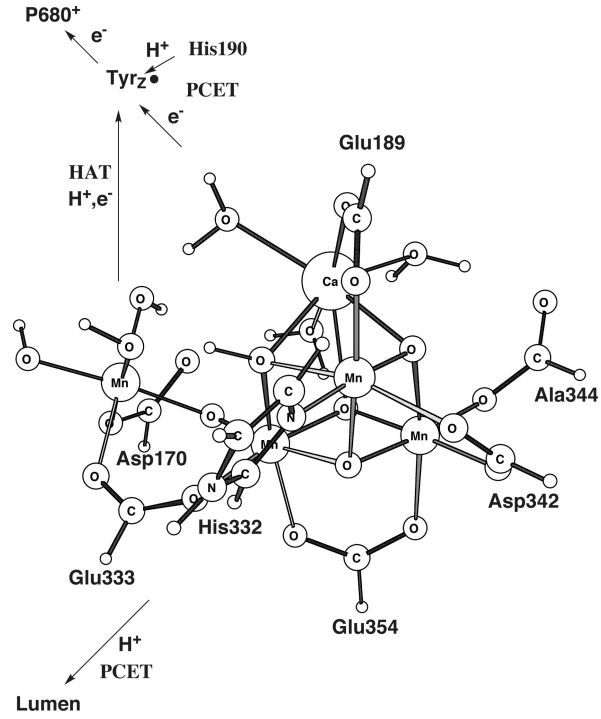

Figure 14. Optimized structure for the S_2 state of the oxygen-evolving complex in photosystem II.[107]

Here, it is assumed that proton release to the lumen would occur already at the stage of Tyr_Z oxidation. The proton would thus not stay at His190. The characteristic feature of the mechanism is that the Tyr_Z radical should act as a hydrogen-atom abstractor from the OEC. The electron should come from the manganese atoms of the OEC and the proton from a substrate water molecule bound at the OEC, just like in the HAT mechanism shown in Figure 1b. From the driving force of the catalytic cycle together with the known bond strengths of water and tyrosine, this HAT hypothesis can be tested.[31] The first reaction of interest is the gas-phase reaction

$$2H_2O \rightarrow O_2 + 4H$$

With an atomization energy of H_2O of 219.3 kcal/mol and a binding energy of O_2 of 118.0 kcal/mol,[105] this reaction is endothermic by 320.6 kcal/mol. Since H_2O is taken from the lumen in PSII, where the binding energy of a H_2O

molecule can be estimated to be 14 kcal/mol, and O_2 is released with an entropy gain of 10 kcal/mol (see section 2), the endergonicity of the actual reaction becomes 338.6 kcal/mol. For a hydrogen-atom abstractor X to give the required exergonicity of the full cycle of 41.5 kcal/mol (see below), the X−H bond strength needs to be (338.6 + 41.5)/4 = 95.0 kcal/mol. However, the O−H bond strength of tyrosine is only 85.8 kcal/mol,[106] indicating that it would not suffice energetically to be a hydrogen-atom abstractor in PSII.

A more general way to realize that it is not optimal to have Tyr_ZO (rad) as a hydrogen-atom abstractor is to divide the process into an electron and a proton transfer. P_{680}^+ has a redox potential of 1.25 V. The electron transfer step from Tyr_Z to P_{680}^+ should ideally be almost isoergonic in order not to lose energy unnecessarily. This means that the redox potential of Tyr_Z should be 1.10 V or higher. This is a higher redox potential than tyrosine normally has, which means that Tyr_Z should be in a positively charged enzyme surrounding that would increase the redox potential. With Tyr_Z in a positive enzyme surrounding it should be a very poor proton acceptor. In fact, since any covalent bond strength like the one in Tyr_ZO-H, is almost unaffected by the enzyme surrounding, an increase of the redox potential due to the surrounding would automatically lead to a corresponding decrease of the pK_a value to a good approximation. It is therefore much more optimal to send the proton to another acceptor than Tyr_Z, in this case directly to the lumen. Hydrogen-atom abstraction is thus not a powerful enough mechanism.

Energy diagrams for the different steps of water oxidation can be obtained in a similar way as described above in section 2 for cytochrome *c* oxidase.[107,108] Using experimental information about the driving force and a single adjustable parameter, accurate pK_a values and redox potentials can be obtained without explicitly describing the enzyme surrounding the active site. The driving force for the catalytic cycle is obtained as 41.5 kcal/mol by using the redox potential for P_{680}^+ of 1.25 V and for oxygen of 0.80 V. The resulting diagram is shown in Figure 15. S_n^m means that *n* is the number of the S state and *m* is the charge of the complex (only including direct ligands to the OEC).

A general comment can first be made about the diagrams, and this is that the protons and electrons are removed in an alternating fashion. This has been the case also in all the previous investigations where energy diagrams were given, see, for example, ref 109. This preserves the charge of the catalyst as much as possible, which has been found to be an energetic advantage in enzyme mechanisms in general.[28] More recently, the model with alternating removal of charges has been used also experimentally to analyze water oxidation in PSII and has been found to explain a large body of experimental results.[110] The general shape of the energy diagram can be described as follows. The first two S transitions are quite exergonic by 24.9 and 8.8 kcal/mol, while the third one from S_2 to S_3 is actually calculated to be slightly endergonic by 0.5 kcal/mol. It is clear that the latter value is not entirely correct since all S transitions must be exergonic. The reason for this is not completely clear at the present stage but could be due to a remaining error in the structure. The key steps in water oxidation occurs in the next transitions. First, formation of an oxygen radical in S_4 is endergonic by 4.9 kcal/mol, which means that this S state will not be observed. O−O bond formation occurs between

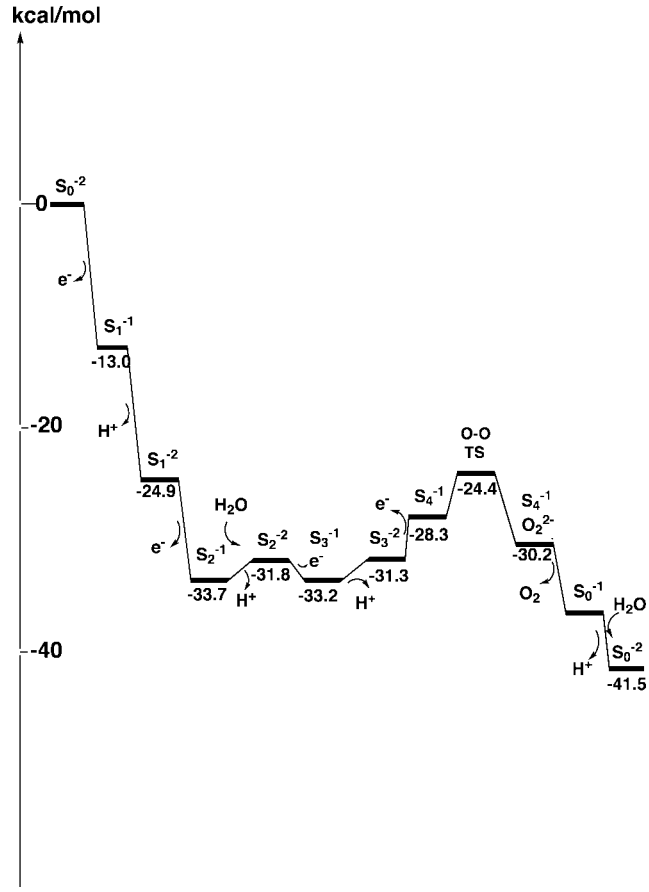

Figure 15. Energy diagram for dioxygen formation in PSII.

the oxygen radical and a bridging oxo ligand of the OEC,[111] with a computed barrier of only 3.9 kcal/mol.[108] This means that the total barrier for O−O bond formation is 3.9 + 4.9 = 8.8 kcal/mol, which is well below what is required for a process that takes milliseconds. The transition from S_3 to S_0 is found to be exergonic by 10.5 kcal/mol.

Since HAT to Tyr_Z appears to be unlikely, the question arises why this electron transfer cofactor is placed in between P_{680} and the OEC. One reason is rather obvious. If the OEC would be placed in direct electron transfer contact with P_{680}, there is a large risk for a shortcut. The electron from the charge separation at P_{680} could then reduce the OEC rather than the quinone Q_A. By having a neutral Tyr_Z on the electron transfer pathway a simple shortcut is no longer possible, since the reduction of a neutral tyrosine is energetically quite unfavorable. Still, a reversal of the previous S transition could, in principle, create a tyrosyl radical that could accept the electron from the charge separation at P_{680} and send it further to the OEC. However, this process would be too slow on the time scale of water oxidation, which is on the order of milliseconds.

The second role of Tyr_Z is more directly related to the water oxidation at the OEC. With a reasonable redox potential of Tyr_Z of 1.1 V, there will be an energy loss in the electron transfer to P_{680}^+ in the first two S transitions, which does not matter since these transitions are so easy energetically. This is not the case for the final two S transitions. From the energy diagram in Figure 15 it can be seen that only an electron is released in the S_1 to S_2 transition. This means that there is a proton remaining on the OEC in S_2 at the stage when Tyr_Z is oxidized. This is also a well-established experimental fact.[112,113] With an electrostatic

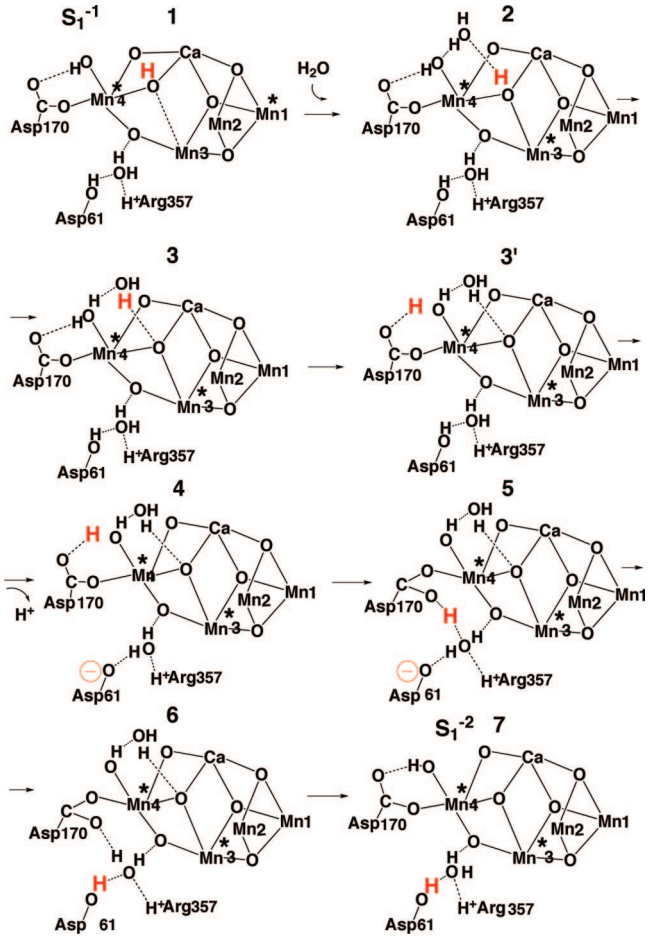

Figure 16. Schematic picture of proton release in the S_1 state. The proton moving in the next step is colored in red, and the manganese atoms in the Mn(IV) state are marked with an asterisk. The other manganese atoms are in the Mn(III) state.

effect from this proton, the redox potential of Tyr_Z will be raised and there will no longer be any energy loss in the later transitions, where the energy is much more needed.

The details of proton transfer has recently been investigated for proton release in the S_1 to S_2 transition,[114] see Figure 16. As seen in this figure the apparently simple release of a proton from a metal complex can be quite complicated. The details will not be discussed here, but a few comments will be given on what is characteristic for this type of process. First, a water molecule has to be added between **1** and **2** to perform the first step in the proton transfer. This does not mean that the water molecule should necessarily be present in this position in the starting structure. If not, there would be a cost to move the water to this position that can be estimated by considering that water is bound in bulk water by about 14 kcal/mol (see section 2). This cost should then be added to the computed barrier. Second, in the proton transfer from structure **1** to **2** an internal electron transfer is needed to oxidize Mn3, since this center forms a stronger Mn−O bond after the proton transfer. These are the main aspects, but there are also other more obvious features, like the rotation of carboxylates and formation and cleavage of hydrogen bonds.

5. Ribonucleotide Reductase

Different types of mechanisms for proton-coupled electron transfer in class I ribonucleotide reductase (RNR) have been

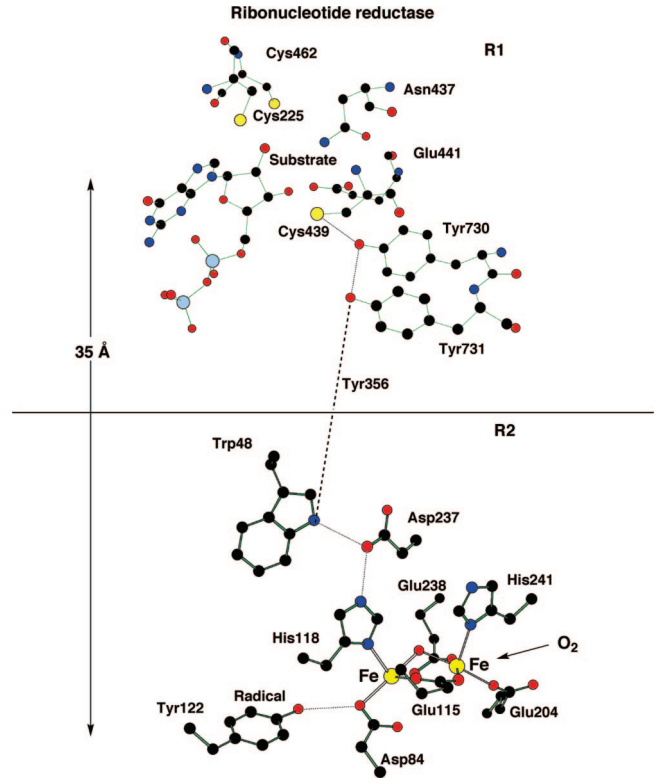

Figure 17. X-ray structure of ribonucleotide reductase. The tyrosyl radical (Tyr122) is created in protein R2, while the substrate reactions occur in R1, 30 Å away.

intensely discussed the past decade. The enzyme is composed of two subunits, R1 where the substrate reactions take place and R2 where an essential tyrosyl radical (Tyr122) is created, see Figure 17.[115,116] The Tyr122 radical in RNR is the first functional amino acid radical identified experimentally in an enzyme.[117] It is a very stable radical which can actually be stored for days. The creation of this radical has obviously attracted a large amount of attention. The current understanding of the steps preceding the creation of this radical can be summarized as follows.[2,118] The Fe_2 (II,II) dimer first binds dioxygen as a peroxide in between the irons, forming a Fe_2 (III,III) complex. As the peroxide is cleaved an electron is transferred from Trp48 (see Figure 17) to the dimer leading to a Fe_2 (IV,III) complex termed compound **X**. The tyrosyl radical is created by reduction of compound **X**, and at that stage a proton may be taken up by one bridging oxo group, leading to an iron dimer structure such as the one shown in Figure 18.[8] In another theoretical study it was shown that the structure of **X** is likely to be slightly different.[119] Instead of only one deprotonated bridging oxygen, both were suggested to be deprotonated.

The distance between Tyr122 and the substrate is over 30 Å. A major point of interest concerns the question of how the radical can move from Tyr122 to the substrate active site without any obvious intermediate redox centers. At an early stage, HAT was advocated for part of this transfer, the one in R1, based on theoretical model studies.[5] This was at the time an entirely new form of long-range radical transfer. In all previously known forms of radical transfer, more or less pure electron transfer was the known mechanism. In two other unusual cases discovered later, electron transfer is still the most plausible mechanism, the one of DNA lyase, where the radical is transferred via tryptophanes, see Figure 1d,[120] and in DNA, where the radical is transferred via

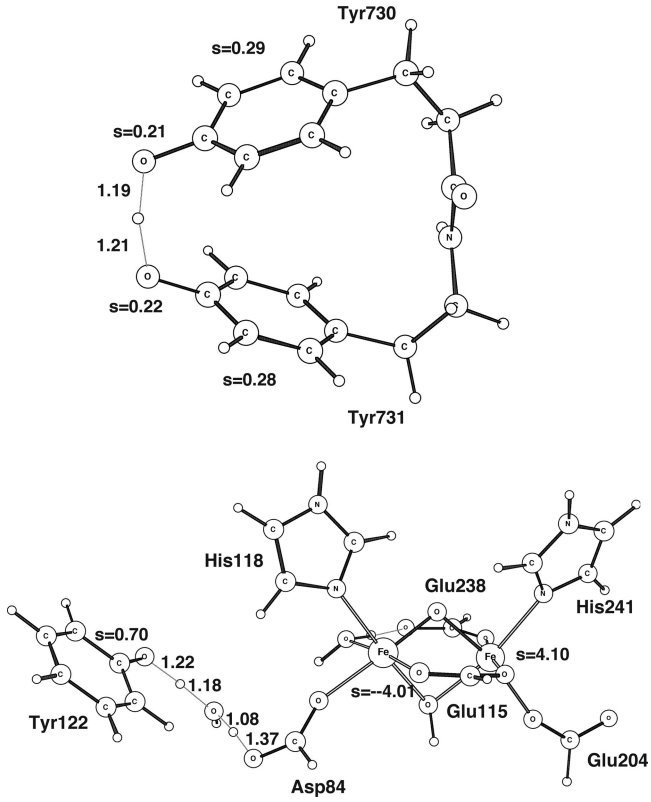

Figure 18. Hydrogen-atom transfer between Tyr730 and Tyr731 in RNR (top) and between tyrosine and compound **X** (bottom). Bond distances (Å) and spins are given in bold.

guanines.[121,122] In both cases there is a hopping mechanism between different centers, as always when there are several cofactors in the radical transfer chain, a very common situation in biology (for example, see cytochrome oxidase discussed above).

A striking feature of the X-ray structure of RNR is that Tyr122 and the substrate site are connected through a hydrogen-bonding network (marked with a dashed line in Figure 17).[118] Some of these hydrogen bonds turn out to be necessary for fast radical transfer. Experiments have shown that when Tyr730 or Tyr731 is mutated to phenylalanine the radical transfer stops.[123] This is the first time a single hydrogen bond has been shown to have such a dramatic effect on electron transfer, which suggests that the mechanism is unusual. An explanation for the mutant experiment came with the realization that the radical transfer between Tyr730 and Tyr731 could be of the type shown in Figure 1a.[5] The computed HAT transition state for a model of the two tyrosines in RNR is shown in Figure 18. The barrier is only 5 kcal/mol, which means that the rate should be on the order of nanoseconds. However, due to the self-interaction error in DFT, these barriers could be underestimated by a few kcal/mol.[124] At the TS the spin is equally distributed on the two tyrosines, about 0.3 on the aromatic rings and 0.2 on the oxygens. As usual in the HAT mechanism there is no spin on the hydrogen that moves, indicating that a strict literal interpretation of HAT should not be made. A similar TS can be located for HAT between Cys439 and Tyr730 with a barrier of 8 kcal/mol corresponding to a rate faster than microseconds. A characteristic general feature of the HAT mechanism is a very small solvent dependence, since there is hardly any charge separation. The estimated effect of the protein surrounding on the barrier is only −0.1 kcal/mol for the Tyr−Tyr case and +0.3 kcal/mol for the Tyr−Cys case. A consequence of these small effects is that the rather small models used should be quite adequate. In contrast, a pure electron transfer would give rise to much larger dielectric effects and require significantly larger models for an accurate description. The radical transfer in the R1 protein in RNR (see Figure 17) can thus be explained by the presence of a HAT mechanism. For example, it is quite obvious that the mutation experiment, where one of the tyrosines was replaced by a phenylalanine, would entirely stop radical transfer by the HAT mechanism. In the R2 protein the radical transfer is much more complicated[8] and fits better under the PCET description.

Impressive experimental efforts have been made in order to establish the character of radical transfer in RNR.[9,10] The functions of Tyr356, Tyr730, and Tyr731 were investigated by site-specific replacement with 3-aminotyrosine. It is interesting to note that very similar conclusions could be drawn from these experiments as those suggested by the calculations. In R1 the mechanism for radical transfer is HAT, while in R2 it is PCET.

Another point of interest has been how the Tyr122 radical is generated through the oxidation of the iron dimer by dioxygen. Since the tyrosyl radical is known to be deprotonated, a main question has been how this deprotonation is coupled to electron transfer from tyrosine to the iron dimer. The mechanism suggested is of the type shown in Figure 1b. The electron and proton come from the same donor and reach the same acceptor, even though the motion is not as strongly coupled as the radical transfer in the first example.

Creation of the tyrosyl radical has been studied by quantum chemical calculations[8] using a model as shown in Figure 18. In this process, both an electron and a proton should be transferred from the tyrosine to the iron dimer. Since the distance between the iron dimer and tyrosine is fairly large, a water molecule has to be inserted to bridge this gap. In fact, without this water the computed barrier is far too high. An interesting transition state for transfer of both a proton and an electron was located as shown in Figure 18. The spin on tyrosine has increased to 0.70, indicating that the electron transfer has proceeded more than halfway. The spin on one of the irons has decreased correspondingly. There is no spin on the atoms in between the iron dimer and tyrosine, including the hydrogens that move. Instead, this region shows the progress of proton transfer, which is about halfway at the TS. The computed barrier for the tyrosyl radical formation is 10 kcal/mol, making this transfer quite rapid on the order of microseconds.

The reverse of the creation of the tyrosyl radical in RNR has stood as a model for the HAT mechanism for dioxygen formation in PSII[6] (see also previous section). A proton and an electron were suggested to go from the manganese-containing oxygen evolving complex (OEC) to a tyrosyl radical, Tyr_Z. At the time this mechanism was suggested there was no structure for PSII. As it later turned out, the distance between the OEC and the Tyr_Z radical in PSII is quite similar to the corresponding distance in RNR.[93,94] The reason HAT was suggested was that in this way a costly charge separation would be avoided. A calculation where iron is replaced by manganese in the model in Figure 18 shows that this does not significantly affect the rate of the reaction, which is therefore in principle quite feasible also for PSII. However, there are other reasons, discussed in the previous section, to argue that a HAT mechanism is not likely for PSII, such as an unnecessary loss of oxidative power.[31]

The final example of a proton-coupled electron transfer process in RNR will be taken from the substrate reactions. The conversion of the substrate ribonucleotide to a deoxyribonucleotide is carried out in R1 with the Cys439 radical (see Figure 17) as catalyst. In the suggested rate-limiting step a keto form of the substrate is converted to a protonated radical simultaneously with the formation of a disulfide bond between Cys225 and Cys462.[125] This means that a rather long-range (about 8 Å) electron transfer from the cysteines to the substrate has to occur together with a proton transfer to the substrate from Glu441, which is clearly not a HAT mechanism but a general PCET one. In the TS, the proton is in between the two oxygens of the substrate and Glu441 and the electron is delocalized with spins both on the substrate and the two cysteines 8 Å away. A similar TS has also been obtained for the class III anaerobic RNR,[126] which has only two cysteines in the active site. In that case the electron transfer is from a formate to the substrate, which are 6 Å apart. It should be noted that in both these substrate reactions, an adiabatic treatment has been possible (and necessary) even though they both involve such a long-range electron transfer as 6−8 Å. A diabatic treatment using Marcus theory might have been possible but would be neither more accurate nor simpler in this PCET.

6. Other Examples

In the present section, a few other examples are given of enzymes where coupled proton and electron transfer plays a major role. These examples are similar to the ones discussed above and will therefore be described in less detail. The first example is nitric oxide reduction in cytochrome *c* oxidase. In this case, it has been demonstrated that it is very important to consider the energetics of proton and electron uptake in order to understand the mechanism of the catalytic cycle. The second example is taken from studies on hydrogenases. These enzymes have attracted a large amount of interest recently due to their possible use in making hydrogen fuel from protons and electrons. Finally, a few examples will be given of short-range HAT, which is very common for transition-metal-containing enzymes.

6.1. Nitric Oxide Reduction

Denitrification is an important part of the global nitrogen cycle. In denitrification, occurring in denitrifying bacteria, nitrite is reduced to dinitrogen in several steps involving coupled electron and proton transfer. One of these steps is the reduction of nitric oxide (NO) to nitrous oxide (N_2O), which occurs in nitric oxide reductase (NOR), an enzyme with large similarities to cytochrome oxidase discussed above in section 3. It has been observed that some species of the two enzymes, cytochrome oxidase and nitric oxide reductase, can reduce both substrates, O_2 and NO, and it should be possible to learn more about these proton-coupled electron transfer processes by studying both reactions. In this context it is interesting to note that NOR does not pump protons, and it is different from CcO also in the sense that the electrons and protons are taken up from the same side of the membrane, while for CcO they are taken up from different sides as discussed above (section 3.1). Furthermore, it has been found for one species of cytochrome oxidase that when NO is reduced by this enzyme the protons are taken up from the same side of the membrane as the electrons, in contrast to when O_2 is reduced by the same enzyme,[127]

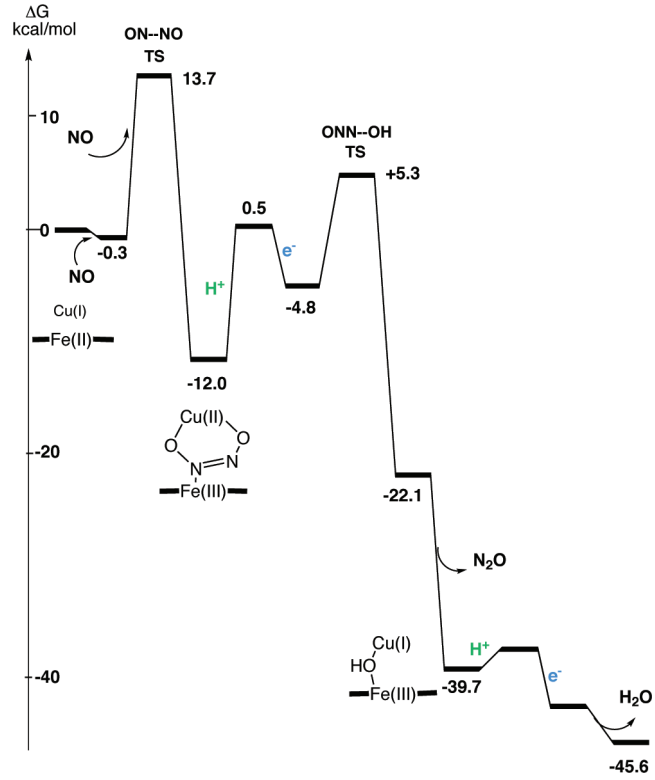

Figure 19. Energetics for the suggested catalytic cycle of NO reduction.

indicating that the details of the coupling between electron and proton transfer is substrate dependent. Since there is no structure available for the bacterial NOR it is more difficult to design models for quantum chemical calculations on this enzyme, but still a few studies have been performed on NO reduction.[128−130] One of these quantum chemical studies is concerned with the NO reduction to N_2O in a ba_3 type of cytochrome oxidase,[128] for which there is a structure available and for which NO reduction has been studied experimentally, yielding a rate-limiting barrier of 19.5 kcal/mol.[131] The reaction studied is thus

$$2\,NO + 2e^- + 2H^+ \rightarrow N_2O + H_2O$$

The model used in the calculations was similar to the central part of the model used for studying O−O bond cleavage in cytochrome oxidase, shown in Figure 11, but without the peripheral residues such as the tyrosine and the water molecules. In contrast to the O_2 reduction, for the case of NO reduction it is not known from experiments at what points of the reaction the protons or electrons enter, and this was therefore one of the questions for the theoretical study. Just as in the case of O_2 reduction discussed above, the cost of electron and proton uptake had to be parametrized to give the overall experimental energy of the reaction, about 46 kcal/mol when heme b is the electron donor. In this case partitioning of the electron and proton cost was fixed by using the experimentally determined difference in reduction potentials for the electron donor (heme b) and the electron acceptor in the second reduction step (heme a_3).

The calculated energy profile for the mechanism for NO reduction found to be most likely is shown in Figure 19. After the first NO molecule has coordinated to iron in the reduced active site the second NO molecule enters and reacts directly with the first one. The N−N bond is formed with a

rather low barrier in a quite stable five-membered ring, see Figure 19. After this step, one of the N−O bonds has to be cleaved, and since a copper−oxo compound is very unstable, it is not possible to cleave any of the N−O bonds without protonating one of the oxygens. The main question is whether only a proton transfer occurs before the bond cleavage or if also an electron is needed. Starting from the protonated five-membered ring it was found that the N−O bond can be cleaved with an intrinsic barrier of 15.5 kcal/mol. However, the total barrier is not possible to obtained without knowing the cost of the protonation step. Furthermore, if an electron is transferred to the protonated five-membered ring, the intrinsic barrier for N−O bond cleavage was found to be lower, only 10.1 kcal/mol. However, in this case the cost of both proton and electron transfer has to be known before the total barrier can be calculated. With the parametrization described above, the proton transfer to the five-membered ring was found to be endergonic by as much as 12.5 kcal/mol, which means that the total barrier for the first mechanism, N−O bond cleavage before electron transfer, became as high as 28 kcal/mol, much higher than the experimental value for the rate-limiting step of the reaction of 19.5 kcal/mol. In contrast, the electron transfer to the protonated five-membered ring turned out to be exergonic by 5.3 kcal/mol, yielding a total barrier of only 17.3 kcal/mol for the mechanism where both proton and electron transfer takes place before the N−O bond cleavage (see Figure 19), compatible with a rate-limiting barrier of 19.5 kcal/mol. This study thus illustrates the importance of taking into account the costs of electron and proton uptake when quantum chemical model calculations are used to study reaction mechanisms for this type of enzymes involving long-range electron and proton transfer.[128]

Finally, the calculated energetics for NO reduction in cytochrome oxidase shown in Figure 19 has been used to speculate about the reason for the lack of electrogenicity and proton pumping observed in one species of cytochrome oxidase when NO is reduced.[127]

6.2. NiFe Hydrogenase

Hydrogenases are also enzymes where coupled transfer of protons and electrons play a major role.[132−134] The most common group of hydrogenases has a NiFe complex at its active site. An X-ray structure from *Desulfomicrobium bacalum* is shown in Figure 20.[135] In the Ni−Fe−Se enzyme in the figure, selenium is substituted for sulfur in one of the cysteine ligands. The NiFe hydrogenases are primarily utilized for hydrogen oxidation, which means that the H−H bond of H_2 is cleaved and the protons and electrons are sent in different directions, as shown in the figure, leading to a charge separation. The electron transfer pathway is easy to identify going over one or more Fe−S cluster. Only the most nearby Fe−S cluster is shown in the figure. A possible proton transfer pathway has been identified, starting at CysSe492, going over Glu23, then over a terminal His498 and Glu51, out to the bulk.[136] Several conserved water molecules bridge these residues.

Hybrid DFT studies to investigate the mechanism of NiFe hydrogenase were initiated already a decade ago.[137−139] These studies considered neither the mechanism nor the energetics of proton or electron release. This was only considered some years later using similar methods as described above.[140] These and other studies are all discussed in a recent review.[141] There was basic agreement on the cleavage mechanism in these

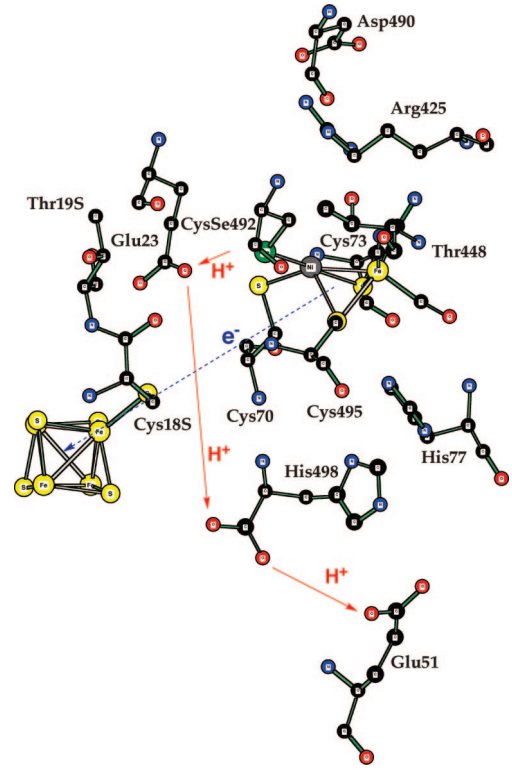

Figure 20. X-ray structure for the reduced form of the [NiFe] hydrogenase from *D. bacalum*.

studies. The reaction starts with the binding of dihydrogen in a local minimum on iron followed by the heterolytic cleavage leading to a hydride bridging between the metals and a proton on one of the cysteines, most likely CysSe492. Rather recently an alternative mechanism was suggested based on DFT calculations.[142] This mechanism starts out like the one described above but with only one not fully completed cycle. After this heterolytic cycle generating a Ni(I) complex, the rest of the catalytic cycles proceed via oxidative addition on nickel generating Ni(III).

For setting up an energy diagram, like the ones above for PSII and CcO, a reference binding energy was needed for the (e^-, H^+) couple that matched a predetermined reaction energy for the whole cycle. In this respect, hydrogenase differs from the enzymes discussed above in the sense that this reaction energy is not known directly from experiments, and a value therefore had to be assumed. Since the enzyme actually can perform the reverse reaction under slightly different circumstances, the reaction energy should be small. For hydrogenase enzymes that work in metabolic processes it is also clear that the driving force should be small under working conditions to minimize the loss of energy. A value of only −1.0 kcal/mol was therefore chosen for the driving force. This is a more uncertain value than the ones for PSII and CcO above but should be qualitatively reasonable. The computed energy diagram for this mechanism is given in Figure 21.

Construction of a complete energy diagram, which includes all steps, is very important for many comparisons to experiments. The most important one is the comparison to the rate of the reaction. The rate of the reaction is determined by the barrier for the rate-limiting step, which starts at the lowest point before the highest barrier. For NiFe hydrogenase, there are three states that have very similar energies. The Ni_a−C* in the diagram is the one that is suggested to

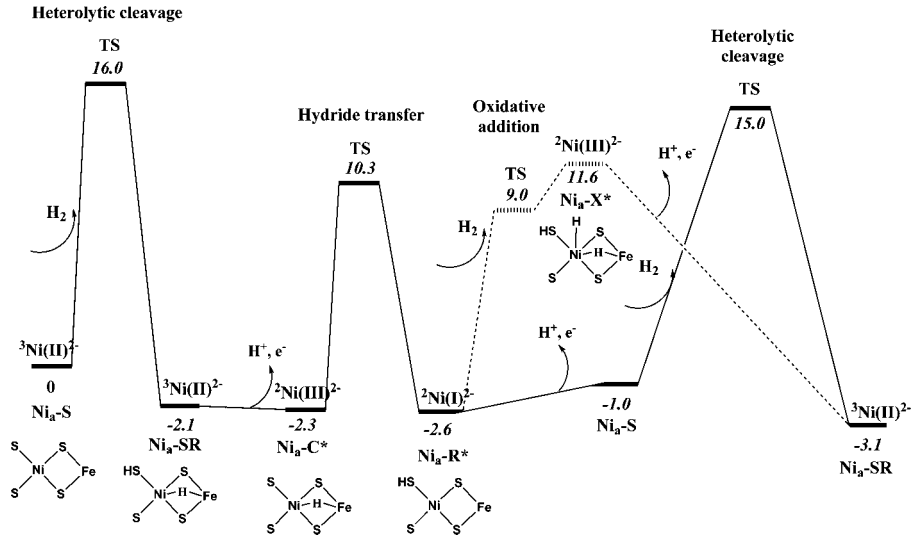

Figure 21. Energetics for the suggested catalytic cycle for Ni−Fe hydrogenase.

be the resting state experimentally. The highest point after that is the H−H bond cleavage in the next cycle, where the energy diagram shows a preference for the oxidative addition rather than the heterolytic mechanism. The rate is thus not determined by the internal barrier for dihydrogen cleavage only, as might have been expected. Identification of the resting state also depends on access to the full energy diagram, since otherwise it would not be possible to determine which state is lowest in energy.

To realize the simplicity of the above scheme for obtaining an energy diagram, it should be compared to the alternative approach. In that approach the electron affinity of the FeS cluster has to be obtained in order to get the electron transfer energy. This is a property which is very sensitive to the enzyme surrounding the complex and therefore has to include a modeling of a major part of the enzyme. The electron affinity of the NiFe complex also has to be computed in a similar way. These two calculations have to be perfectly balanced in order to compute the electron transfer energy. It should be added that not even this may be enough, since the one with the lowest energy of the electron acceptors may not be the first FeS cluster in the electron transfer chain. The other ones should therefore also be computed. The proton transfer energy is even more difficult to obtain in this way. The accuracy of the present approach is instead mainly limited by the computed local chemistry, such as the exergonicity of the cleavage of H_2. An error in that energy would transfer directly to the computed redox potentials and pK_a values. The loss of accuracy by introducing just an estimated value for the reaction energy should be a much less severe approximation in this context.

6.3. Short-Range PCET

The examples discussed above have all been for enzymes where long-range PCET plays a dominant role. In the present subsection a few examples will be mentioned where the PCET is much more short range. These are very common in redox-active enzymes, which means that a complete picture cannot be given. Most of them will in the present nomenclature be called HAT. Some typical examples, involving methane activation, are shown in Figure 22. Enzymatic hydroxylation of methane has been one of the subjects most intensely studied by theory during the past decade.[143−145] Methane monooxygenases (MMO's) are the only enzymes that can perform this difficult chemical task in nature. Nonheme iron monomers are known to perform hydroxylations of other hydrocarbons,[146] and so are the P450 enzymes.[147]

There is a large group of mononuclear nonheme enzymes that perform C−H activation. Most of these complexes have a two-His−one-carboxylate triad as ligands with remaining positions filled by water-derived ligands. C−H activation is rate limiting for methane but not normally for most other substrates. This step is often preceded by creation of a Fe(IV)═O complex by reaction with oxygen. The transition-state geometry always has the carbon, hydrogen, and oxygen atoms on an almost straight line. In the C−H cleavage step, a proton is transferred from the substrate to the oxo group while the electron goes from the substrate to the d orbitals of iron, the reverse of case b in Figure 1. There will be no spin on hydrogen at the TS.

The C−H activation step is rather similar for compound Q of MMO. This is an Fe_2 (IV,IV) complex, which is created by a reaction with oxygen and is one of the most powerful oxidants in biology. Again, the carbon, hydrogen, and oxygen atoms are on an almost straight line in the TS. The C−H activation is preceded by a change of state of the complex to a Fe_2 (III,V) state, which can also be described as a Fe_2 (III,IV) complex with a bridging oxygen radical. The proton goes to the bridging oxygen, and depending on which resonance state is used, the electron will go from the substrate to the oxygen radical or to the Fe(V) atom. In the former case the C−H activation can be described as a quite clean case of HAT. The second iron, the Fe(III) atom, is passive during the C−H activation.

C−H activation is slightly different for compound I of the P450 family of enzymes. This complex has again an Fe(IV) center but also a porphyrin radical slightly delocalized on the cysteine. The ligand field is strong, leading to a low-spin Fe(IV), which will couple to the porphyrin radical as either a doublet or a quartet. In the HAT C−H activation step the proton goes to the oxo ligand, as in the cases described above, but now the electron goes to the porphyrin radical. The hydroxylation of the substrate can be different depending on the state, doublet or quartet, and the term two-state reactivity has been used to describe this situation.[147] In compound II, which is reduced by one electron compared to compound I, there is no radical on the porphyrin, and this

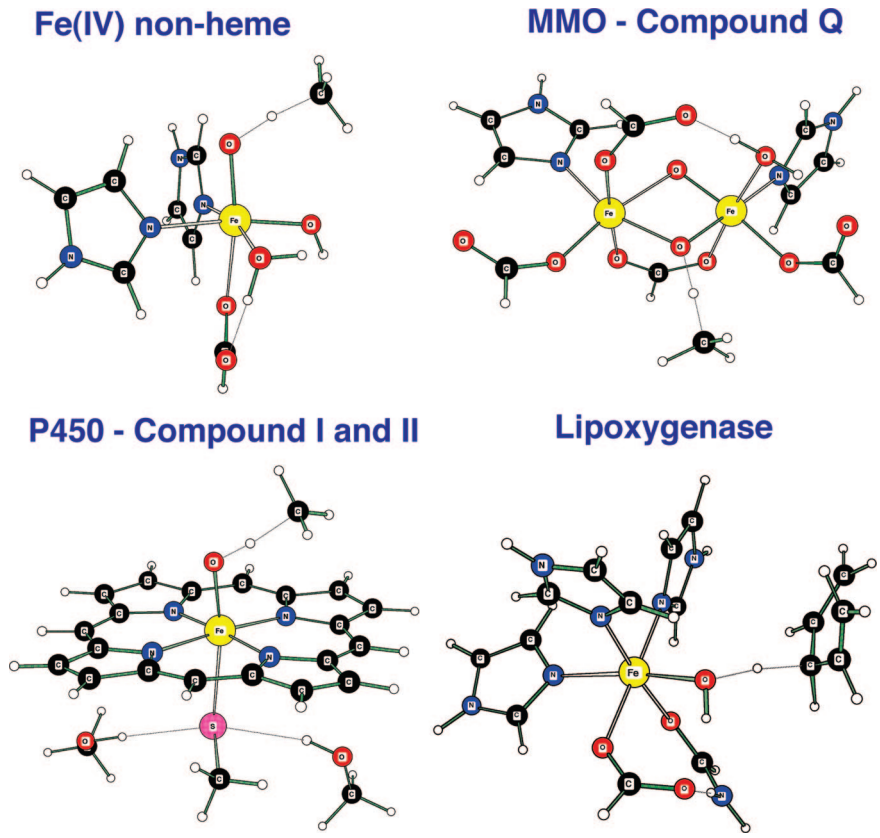

Figure 22. Hydrogen-atom transfer in four cases discussed in the text.

compound is therefore substantially less reactive. In the HAT C−H activation, the electron now goes to the iron center, reducing it to Fe(III).

The final example discussed here is for soybean lipoxygenase (SLO). This is a mononuclear Fe(III) complex, which has attracted a large amount of interest since an unusually large kinetic isotope effect of 81 has been found experimentally.[148] Furthermore, the temperature dependences of the rate and KIE were found to be quite weak. In the rate-limiting step a hydrogen atom is transferred from the lineolic acid substrate, creating a radical, to the Fe(III)−OH ligand, creating a Fe(II)−H_2O complex. This complex is thus different from the ones discussed above, where the much stronger oxidant Fe(IV) was involved, which is possible because of the high stability of the substrate radical leading to a weak C−H bond. To describe the unusual KIE and the temperature dependence, nuclear quantum mechanical (NQM) effects need to be considered. This has been done in two quite different ways. In the first of these studies, a quantum classical path (QCP) approach was used.[149] The second study instead used a diabatic multistate dielectric continuum theory of PCET.[150] Both studies managed to obtain a very high degree of agreement with experiments.

7. Summary

In the present review, quantum chemical descriptions of PCET in metalloenzymes have been discussed. The most common type of PCET occurring in enzymes is of the two-step type, where the electron and proton move in separate steps and where the electron and proton have different donors and acceptors. The enzymes discussed here of that type are characterized by the uptake (or release) of electrons and protons from (to) the outside of the enzyme, and this type of long-range electron and proton transfer typically occurs in several steps of PCET. It has been shown how quantum chemical methods can be used to increase the understanding of the mechanisms for these quite complicated types of processes. An important aspect has been how a combination of calculated relative energies and experimental redox potentials can be used to obtain reliable energies for the intermediates.

The two enzymes most thoroughly discussed here are cytochrome *c* oxidase (CcO) and photosystem II (PSII), involving the reduction of molecular oxygen to water, or the reverse reaction of water oxidation with the formation of molecular oxygen. Both these reactions occur in four steps, each comprising the uptake (or release) of one electron and one proton. In the case of CcO, each of the reduction steps is coupled to the translocation of another proton across the entire membrane (in which the enzyme is located). The fact that this pumping occurs without major structural changes or involvement of ATP but is only governed by the electrostatic effects of moving the electrons may make it unique in biology. It was discussed how quantum chemical calculations could be used to elucidate the mechanisms for this complicated coupling of the electron and proton transfer leading to a gating of the protons to the desired place in each step. Another important enzyme discussed is ribonucleotide reductase (RNR), where quantum chemical studies have shown that several different types of PCET occur. In particular, RNR seems to be the most clear case for which hydrogen-atom transfer (HAT) is involved in long-range radical transfer, with the electron and proton being transferred between the same donor and acceptor molecule (two tyrosines or a cysteine and a tyrosine).

The QM models used for quantum chemical studies of PCET processes have grown over the past two decades from about 20 atoms to the present 250 atoms. Increasing the size

of the models leads to additional difficulties, such as the presence of many local minima, which is at the present stage a major challenge in the modeling. It can be expected that the growing experience with large models will lead to still better treatments of this local minima problem in the future. However, it should be stressed that very large models are not needed, not even desired, for all types of problems. It can be predicted that also in the future the main features of most PCET mechanisms will be elucidated using rather small models. Extended models can then be used to make the mechanisms found with the small models more convincing.

9. References

(1) Huynh, M. H. V.; Meyer, T. J. *Chem. Rev.* **2007**, *107*, 5004.
(2) Stubbe, J.; van der Donk, W. A. *Chem. Rev.* **1998**, *98*, 705.
(3) Himo, F.; Siegbahn, P. E. M. *Chem. Rev.* **2003**, *103*, 2421.
(4) Himo, F. *Biochim. Biophys. Acta* **2005**, *1707*, 24.
(5) Siegbahn, P. E. M.; Eriksson, L.; Himo, F.; Pavlov, M. *J. Phys. Chem.* **1998**, *102*, 10622.
(6) Babcock, G. T. The oxygen-evolving complex in photosystem II as a metallo-radical enzyme. In *Photosynthesis from Light to Biosphere*; Mathis, P., Ed.; Kluwer: Dordrecht, The Netherlands, 1995; Vol. 2, p 209.
(7) Meyer, J. M.; Hrovat, D. A.; Thomas, J. L.; Borden, W. T. *J. Am. Chem. Soc.* **2002**, *124*, 11142.
(8) Siegbahn, P. E. M. *Q. Rev. Biophys.* **2003**, *36*, 91.
(9) Stubbe, J.; Nocera, D. G.; Yee, C. S.; Chang, M. C. Y. *Chem. Rev.* **2003**, *98*, 2167.
(10) Seyedsayamdost, M. R.; Xie, J.; Chan, C. T. Y.; Schultz, P. G.; Stubbe, J. *J. Am. Chem. Soc.* **2007**, *129*, 15060.
(11) Hammes-Schiffer, S.; Soudackov, A. V. *J. Phys. Chem. B* **2008**, *112*, 14108.
(12) Georgievskii, Y.; Stuchebrukhov, A. A. *J. Chem. Phys.* **2000**, *113*, 10438.
(13) Cukier, R. I. *J. Phys. Chem.* **1994**, *98*, 2377.
(14) Marcus, R. A. *Annu. Rev. Phys. Chem.* **1964**, *15*, 155.
(15) Liu, H.; Warshel, A. *J. Phys. Chem. B* **2007**, *111*, 7852.
(16) Hay, S.; Johannissen, L. O.; Sutcliffe, M. J.; Scrutton, N. S. *Biophys. J.* **2010**, *98*, 121.
(17) Kamerlin, S. C. L.; Warshel, A. *J. Phys. Org. Chem.* **2010**, DOI 10.1002/poc.1620.
(18) Page, C. C.; Moser, C. C.; Chen, X. X.; Dutton, P. L. *Nature* **1999**, *402*, 47.
(19) Gray, H. B.; Winkler, J. R. *Q. Rev. Biophys.* **2003**, *36*, 341.
(20) Moser, C. C.; Anderson, J. L. R.; Dutton, P. L. *Biochim. Biophys. Acta* **2010**, *1797*, 1573.
(21) Becke, A. D. *J. Chem. Phys.* **1993**, *98*, 5648.
(22) Siegbahn, P. E. M. *J. Biol. Inorg. Chem.* **2006**, *11*, 695.
(23) Warshel, A.; Levitt, M. *J. Mol. Biol.* **1976**, *103*, 227.
(24) Senn, H. M.; Thiel, W. *Top. Curr. Chem.* **2007**, 268.
(25) Siegbahn, P. E. M.; Himo, F. *J. Biol. Inorg. Chem.* **2009**, *14*, 643.
(26) Siegbahn, P. E. M.; Blomberg, M. R. A.; Blomberg, M. L. *J. Phys. Chem. B* **2003**, *107*, 10946.
(27) Blomberg, M. R. A.; Siegbahn, P. E. M. *J. Comput. Chem.* **2006**, *27*, 1373.
(28) Siegbahn, P. E. M.; Blomberg, M. R. A. In *Computational Modeling for Homogeneous Catalysis and Biocatalysis*; Morokuma, K., Musaev, J., Eds.; Wiley-VCH: Germany, 2008; p 57.
(29) Siegbahn, P. E. M.; Blomberg, M. R. A. *Dalton Trans.* **2009**, 5832.
(30) Blomberg, M. R. A.; Siegbahn, P. E. M. *Biochim. Biophys. Acta* **2010**, *1797*, 129.
(31) Siegbahn, P. E. M. *Proc. R. Soc.* **2008**, *363*, 1221.
(32) Siegbahn, P. E. M.; Blomberg, M. R. A. *J. Phys. Chem A* **2008**, *112*, 12772.
(33) Morgan, J. E.; Verkhovsky, M. I.; Wikström, M. *J. Bioenerg. Biomembr.* **1994**, *26*, 599. Wikström, M.; Morgan, J. E.; Verkhovsky, M. I. *J. Bioenerg. Biomembr.* **1998**, *30*, 139. Wikström, M. *Biochim. Biophys. Acta* **2000**, *44827*, 1.
(34) Michel, H. *Proc. Natl. Acad. Sci. U.S.A.* **1998**, *95*, 12819. Michel, H. *Biochemistry* **1999**, *38*, 15129. Ruitenberg, M.; Kannt, A.; Bamberg, E.; Fendler, K.; Michel, H. *Nature* **2002**, *417*, 99.
(35) Gennis, R. B. *Proc. Natl. Acad. Sci. U.S.A.* **1998**, *95*, 12747.
(36) Mitchell, R.; Rich, P. R. *Biochim. Biophys. Acta* **1994**, *1186*, 19.
(37) Capitanio, N.; Vygodina, T. V.; Capitanio, G.; Konstantinov, A. A.; Nicholls, P.; Papa, S. *Biochim. Biophys. Acta* **1997**, *1318*, 255.
(38) Blair, D. F.; Ellis, J.; Walther, R.; Wang, H.; Gray, H. B.; Chan, S. I. *J. Biol. Chem.* **1986**, *261*, 1524.
(39) Carithers, R. P.; Palmer, G. *J. Biol. Chem.* **1981**, *256*, 7967.
(40) Artzatbanov, V. Y.; Konstantinov, A. A.; Skulachev, V. P. *FEBS Lett.* **1978**, *87*, 180.
(41) Brzezinski, P.; Larsson, G. *Biochim. Biophys. Acta* **2003**, *1605*, 1.
(42) Faxen, K.; Gilderson, G.; Ädelroth, P.; Brzezinski, P. *Nature* **2005**, *437*, 286.
(43) Song, Y.; Michonova-Alexova, E.; Gunner, M. R. *Biochemistry* **2006**, *45*, 7959.
(44) Popovic, D. M.; Stuchebrukhov, A. A. *J. Am. Chem. Soc.* **2004**, *126*, 1858.
(45) Popovic, D. M.; Stuchebrukhov, A. A. *FEBS Lett.* **2004**, *566*, 126.
(46) Medvevev, D. M.; Medvevev, E. S.; Kotelnikov, A. I.; Stuchebrukhov, A. A. *Biochim. Biophys. Acta* **2005**, *1710*, 47.
(47) Popovic, D. M.; Stuchebrukhov, A. A. *J. Phys. Chem. B* **2005**, *109*, 1999.
(48) Fadda, E.; Yu, C.-H.; Pomes, R. *Biochim. Biophys. Acta* **2008**, *1777*, 277.
(49) Quenneville, J.; Popovic, D. M.; Stuchebrukhov, A. A. *J. Phys. Chem. B* **2005**, *108*, 18383.
(50) Popovic, D. M.; Quenneville, J.; Stuchebrukhov, A. A. *J. Phys. Chem. B* **2005**, *109*, 3616.
(51) Makhov, D. V.; Popovic, D. M.; Stuchebrukhov, A. A. *J. Phys. Chem. B* **2006**, *110*, 12162.
(52) Stuchebrukhov, A. A.; Popovic, D. M. *J. Phys. Chem. B* **2006**, *110*, 17286.
(53) Quenneville, J.; Popovic, D. M.; Stuchebrukhov, A. A. *Biochim. Biophys. Acta* **2006**, *1757*, 1035.
(54) Fadda, E.; Chakrabarti, N.; Pomes, R. *J. Phys. Chem. B* **2005**, *109*, 22629.
(55) Fadda, E.; Chakrabarti, N.; Pomes, R. *J. Phys. Chem. B* **2006**, *110*, 17288.
(56) Olsson, M. H.; Sharma, P. K.; Warshel, A. *FEBS Lett.* **2005**, *579*, 2026.
(57) Olsson, M. H.; Warshel, A. *Proc. Natl. Acad. Sci. U.S.A.* **2006**, *103*, 6500.
(58) Olsson, M. H.; Siegbahn, P. E. M.; Blomberg, M. R. A.; Warshel, A. *Biochim. Biophys. Acta* **2007**, *1767*, 244.
(59) Henry, R. M.; Yu, C.-H.; Rodinger, T.; Pomes, R. *J. Mol. Biol.* **2009**, *387*, 1165.
(60) Siegbahn, P. E. M.; Blomberg, M. R. A. *Biochim. Biophys. Acta* **2007**, *1767*, 1143.
(61) Verkhovsky, M. I.; Wikström, M. *Biochim. Biophys. Acta* **2007**, *1767*, 1200.
(62) Kaila, V. R. I.; Verkhovsky, M.; Hummer, G.; Wikström, M. *Biochim. Biophys. Acta* **2009**, *1787*, 1205.
(63) Kaila, V. R. I.; Verkhovsky, M.; Hummer, G.; Wikström, M. *Biochim. Biophys. Acta* **2008**, *1777*, 890.
(64) Kaila, V. R. I.; Verkhovsky, M.; Hummer, G.; Wikström, M. *Proc. Natl. Acad. Sci. U.S.A.* **2008**, *105*, 6255.
(65) Wikström, M.; Verkhovsky, M.; Hummer, G. *Biochim. Biophys. Acta* **2003**, *1604*, 61.
(66) Kim, Y. C.; Wikström, M.; Hummer, G. *Proc. Natl. Acad. Sci. U.S.A.* **2009**, *106*, 13707.
(67) Blomberg, M. R. A.; Siegbahn, P. E. M. *Mol. Phys.*, in press.
(68) Belevich, I.; Bloch, D. A.; Belevich, N.; Wikström, M.; Verkhovsky, M. I. *Proc. Natl. Acad. Sci. U.S.A.* **2007**, *104*, 2685.
(69) Moore, D. B.; Martinez, T. J. *J. Phys. Chem. A* **2000**, *104*, 2367.
(70) Kaukonen, M. *J. Phys. Chem. B* **2007**, *111*, 12543.
(71) Fee, J. A.; Case, D. A.; Noodleman, L. *J. Am. Chem. Soc.* **2008**, *130*, 15002.
(72) Brzezinski, P. *Trends Biochem. Sci.* **2004**, *29*, 380.
(73) Wikström, M. *Biochim. Biophys. Acta* **2004**, *1655*, 241.
(74) Yoshioka, Y.; Kawi, H.; Yamaguchi, K. *Chem. Phys. Lett.* **2003**, *374*, 45.
(75) Mitani, M.; Inoue, M.; Yoshioka, Y. *Chem. Phys. Lett.* **2007**, *440*, 296.
(76) Yoshioka, Y.; Satoh, H.; Mitani, M. *J. Inorg. Biochem.* **2007**, *101*, 1410.
(77) Ghosh, A.; Skancke, A. *J. Phys. Chem. B* **1998**, *102*, 10087.
(78) Daskalakis, V.; Pinakoulaki, E.; Stavrakis, S.; Varotsis, C. *J. Phys. Chem. B* **2007**, *111*, 10502.
(79) Daskalakis, V.; Farantos, S. C.; Varotsis, C. *J. Am. Chem. Soc.* **2008**, *130*, 12385.
(80) Colbran, S. B.; Paddo-Row, M. N. *J. Biol. Inorg. Chem.* **2003**, *8*, 855.
(81) Kaila, V. R. I.; Johansson, M. P.; Sundholm, D.; Laakkonen, L.; Wikström, M. *Biochim. Biophys. Acta* **2009**, *1787*, 221.
(82) Kamiya, K.; Boero, M.; Tateno, M.; Shiraishi, K.; Oshiyama, A. *J. Am. Chem. Soc.* **2007**, *129*, 9663.
(83) Blomberg, M. R. A.; Siegbahn, P. E. M.; Babcock, G. T.; Wikström, M. *J. Inorg. Biochem.* **2000**, *80*, 261.
(84) Blomberg, M. R. A.; Siegbahn, P. E. M.; Babcock, G. T.; Wikström, M. *J. Am. Chem. Soc.* **2000**, *122*, 12848.

(85) Blomberg, M. R. A.; Siegbahn, P. E. M.; Wikström, M. *Inorg. Chem.* **2003**, *42*, 5231.
(86) Hansson, Ö.; Karlsson, B.; Aasa, R.; Vänng aard, T.; Malmsröm, B. G. *EMBO J.* **1992**, *1*, 1295.
(87) Proshlyakov, D. A.; Pressler, M. A.; Babcock, G. T. *Proc. Natl. Acad. Sci. U.S.A.* **1998**, *95*, 8020.
(88) Karpefors, M.; Ädelroth, P.; Namslauer, A.; Zhen, Y.; Brzezinski, P. *Biochemistry* **2000**, *39*, 14664.
(89) Kannt, A.; Lancaster, R. D.; Michel, H. *Biophys. J.* **1998**, *74*, 708.
(90) Tuukkanen, A.; Verkhovsky, M. I.; Laakkonen, L.; Wikström, M. *Biochim. Biophys. Acta* **2006**, *1757*, 1117.
(91) Bränden, M.; Sigurdson, H.; Namslauer, A.; Gennis, R.; Ädelroth, P.; Brzezinski, P. *Proc. Natl. Acad. Sci. U.S.A.* **2001**, *98*, 5013.
(92) Qin, L.; Liu, J.; Mills, D. A.; Proshlyakov, D. A.; Hiser, C.; Ferguson-Miller, S. *Biochemistry* **2009**, *48*, 5121.
(93) Ferreira, K. N.; Iverson, T. M.; Maghlaoui, K.; Barber, J.; Iwata, S. *Science* **2004**, *303*, 1831.
(94) Loll, B.; Kern, J.; Saenger, W.; Zouni, A.; Biesiadka, J. *Nature* **2005**, *438*, 1040.
(95) Guskov, A.; Kern, J.; Gabdulkhakov, A.; Broser, M.; Zouni, A.; Saenger, W. J. *Nat. Struct. Biol.* **2009**, *16*, 334.
(96) Siegbahn, P. E. M. *Chem.—Eur. J.* **2008**, *27*, 8290.
(97) Sproviero, E. M.; Gascon, J. A.; McEvoy, J. P.; Brudvig, G. W.; Batista, V. S. *J. Am. Chem. Soc.* **2008**, *130*, 3428–3442. Sproviero, E. M.; Gascon, J. A.; McEvoy, J. P.; Brudvig, G. W.; Batista, V. S. *J. Am. Chem. Soc.* **2008**, *130*, 6728.
(98) Pantazis, D. A.; Orio, M.; Petrenko, T.; Zein, S.; Lubitz, W.; Messinger, J.; Neese, F. *Phys. Chem. Chem. Phys.* **2009**, *11*, 6788.
(99) Yano, J.; Kern, J.; Sauer, K.; Latimer, M. J.; Pushkar, Y.; Biesiadka, J.; Loll, B.; Saenger, W.; Messinger, J.; Zouni, A.; Yachandra, V. K. *Science* **2006**, *314*, 821. Yano, J.; Kern, J.; Pushkar, Y.; Sauer, K.; Glatzel, P.; Bergmann, U.; Messinger, J.; Zouni, A.; Yachandra, V. K. *Philos. Trans. R. Soc. B* **2008**, *363*, 1139.
(100) Siegbahn, P. E. M. *J. Am. Chem. Soc.* **2009**, *131*, 18238.
(101) Ishikita, H.; Knapp, E.-W. *J. Biol. Chem.* **2005**, *280*, 12446.
(102) Diner, B. A. *Biochim. Biophys. Acta* **2001**, *1503*, 147.
(103) Rappaport, F.; Lavergne, J. *Biochim. Biophys. Acta* **2001**, *1503*, 246.
(104) Ahlbrink, R.; Haumann, M.; Cherepanov, D.; Bögershausen, O.; Mulkidjanian, A.; Junge, W. *Biochemistry* **1998**, *37*, 1131.
(105) Curtiss, L. A.; Raghavachari, K.; Trucks, G. W.; Pople, J. A. *J. Chem. Phys.* **1991**, *94*, 7221.
(106) Kerr, J. A. *Handbook of Chemistry and Physics*, 77th ed.; Chemical Rubber Company: Cleveland, 1996; p 9.
(107) Siegbahn, P. E. M. *Acc. Chem. Res.* **2009**, *42*, 1871.
(108) Siegbahn, P. E. M. In *Molecular Solar Fuels*; Wydrzynski, T. J., Hillier, W., Eds.; RSC Publishing: Cambridge, England, in press.
(109) Siegbahn, P. E. M.; Lundberg, M. *Photochem. Photobiol. Sci.* **2005**, *4*, 1035.
(110) Dau, H.; Haumann, M. *Biochim. Biophys. Acta* **2007**, *1767*, 472.
(111) Siegbahn, P. E. M. *Chem.—Eur. J.* **2006**, *12*, 9217.
(112) Renger, G. *Physiol. Plant.* **1997**, *100*, 828.
(113) Förster, V.; Junge, W. *Photochem. Photobiol.* **1985**, *41*, 183.
(114) Siegbahn, P. E. M. *Dalton Trans.* **2009**, 10063.
(115) Eriksson, M.; Uhlin, U.; Ramaswamy, S.; Ekberg, M.; Regnström, K.; Sjöberg, B.-M.; Eklund, H. *Structure* **1997**, *5*, 1077.
(116) Nordlund, P.; Sjöberg, B.-M.; Eklund, H. *Nature* **1990**, *345*, 593.
(117) Ehrenberg, A.; Reichard, P. *J. Biol. Chem.* **1972**, *247*, 3485.
(118) Sjöberg, B.-M. In *Nucleic Acids and Molecular Biology*; Eckstein, F. Lilley, D. M. J., Eds.; Springer Verlag: 1995; Vol. 9, p 192.
(119) Han, W.-G.; Liu, T.; Lovell, T.; Noodleman, L. *J. Inorg. Biochem.* **2006**, *100*, 771.
(120) Aubert, C.; Vos, M. H.; Mathis, P.; Eker, A. P.; Brettel, K. *Nature* **2000**, *405*, 586.
(121) Boon, E. M.; Barton, J. K. *Curr. Opin. Struct. Biol.* **2002**, *12*, 320.
(122) Giese, B. *Annu. Rev. Biochem.* **2002**, *71*, 51.
(123) Ekberg, M.; Sahlin, M.; Eriksson, M.; Sjöberg, B. M. *J. Biol. Chem.* **1996**, *271*, 20655.
(124) Lundberg, M.; Siegbahn, P. E. M. *J. Chem. Phys.* **2005**, *122*, 224103—1-9.
(125) Pelmenschikov, V.; Cho, K.-B.; Siegbahn, P. E. M. *J. Comput. Chem.* **2004**, *25*, 311.
(126) Cho, K.-B.; Pelmenschikov, V.; Gräslund, A.; Siegbahn, P. E. M. *J. Phys. Chem. B* **2004**, *108*, 2056.
(127) Huang, Y.; Reimann, J.; Lepp, H.; Drici, N.; Ädelroth, P. *Proc. Natl. Acad. Sci. U.S.A.* **2008**, *105*, 20257.
(128) Blomberg, L. M.; Blomberg, M. R. A.; Siegbahn, P. E. M. *Biochim. Biophys. Acta* **2006**, *1757*, 31.
(129) Blomberg, L. M.; Blomberg, M. R. A.; Siegbahn, P. E. M. *Biochim. Biophys. Acta* **2006**, *1757*, 240.
(130) Blomberg, L. M.; Blomberg, M. R. A.; Siegbahn, P. E. M. *J. Biol. Inorg. Chem.* **2007**, *12*, 79.
(131) Giuffre, A.; Stubauer, G.; Sarti, P.; Brunori, M.; Zumft, W. G.; Buse, G.; Soulimane, T. *Proc. Natl. Acad. Sci. U.S.A.* **1999**, *96*, 14718.
(132) Przbyla, A. E.; Robbins, J.; Menon, N.; Peck, H. D., Jr. *FEMS Microbiol. Rev.* **1992**, *88*, 109.
(133) Nicolet, Y.; Lemon, B. J.; Fontecilla-Camps, J. C.; Peters, J. W. *Trends Biochem. Sci.* **2000**, *25*, 138.
(134) Lyon, E. J.; Shima, S.; Buurman, G.; Chowdhuri, S.; Batschauer, A.; Steinbach, K.; Thauer, R. K. *Eur. J. Biochem.* **2004**, *271*, 195.
(135) Garcin, E.; Vernede, X.; Hatchikian, E. C.; Volbeda, A.; Frey, M.; Fontecilla-Camps, J. C. *Structure* **1999**, *7*, 557.
(136) Frey, M.; Fontecilla-Camps, J. C. In *Handbook of Metalloproteins*; Messerschmidt, A., Huber, R., Poulos, T., Wieghardt, K., Eds.; John Wiley & Sons: Chichester, U.K., 2001; Vol. 2, p 880.
(137) Pavlov, M.; Siegbahn, P. E. M.; Blomberg, M. R. A.; Crabtree, R. H. *J. Am. Chem. Soc.* **1998**, *120*, 548.
(138) Niu, S. Q.; Thomson, L. M.; Hall, M. B. *J. Am. Chem. Soc.* **1999**, *121*, 4000.
(139) De Gioia, L.; Fantucci, P.; Guigliarelli, B.; Bertrand, P. *Inorg. Chem.* **1999**, *38*, 2658.
(140) Siegbahn, P. E. M. *Adv. Inorg. Chem.* **2004**, *56*, 101.
(141) Siegbahn, P. E. M.; Tye, J. W.; Hall, M. B. *Chem. Rev.* **2007**, *107*, 4414.
(142) Nilsson Lill, S. O.; Siegbahn, P. E. M. *Biochemistry* **2009**, *48*, 1056.
(143) Baik, M.-H.; Newcombe, M.; Friesner, R. A.; Lippard, S. J. *Chem. Rev.* **2003**, *103*, 2385.
(144) Basch, H.; Mogi, K.; Musaev, D. G.; Morokuma, K. *J. Am. Chem. Soc.* **1999**, *121*, 7249.
(145) Siegbahn, P. E. M. *J. Biol. Inorg. Chem.* **2001**, *6*, 27.
(146) Bassan, A.; Borowski, T.; Siegbahn, P. E. M. *Dalton. Trans.* **2004**, *20*, 3153.
(147) Shaik, S.; Kumar, D.; de Visser, S. P.; Altun, A.; Thiel, W. *Chem. Rev.* **2005**, *105*, 2279.
(148) Knapp, M. J.; Rickert, K. W.; Klinman, J. P. *J. Am. Chem. Soc.* **2002**, *124*, 3865.
(149) Olsson, M. H. M.; Siegbahn, P. E. M.; Warshel, A. *J. Am. Chem. Soc.* **2004**, *126*, 2820–2828. *J. Biol. Inorg. Chem.* **2004**, *9*, 96.
(150) Hatcher, E.; Soudackov, A. V.; Hammes-Schiffer, S. *J. Am. Chem. Soc.* **2007**, *129*, 187. *J. Am. Chem. Soc.* **2004**, *126*, 5763.

CR100070P